



Multiple indices based agricultural drought assessment in the northwestern part of Bangladesh using geospatial techniques

Most. Shahana Sultana, Md. Yousuf Gazi*, Md. Bodruddoza Mia

Department of Geology, University of Dhaka, Dhaka 1000, Bangladesh



ARTICLE INFO

Keywords:

Multivariate drought indices
Agricultural drought
Drought assessment
Geospatial techniques
Bangladesh

ABSTRACT

Droughts are very common in Bangladesh especially in the northwestern part, due to geographical position, variation in Groundwater table, and the spatial variation in seasonal rainfall pattern. In the present study, three drought indices viz., Vegetation Health Index (VHI), Temperature Vegetation Dryness Index (TVDI), and Short-wave Infrared Dryness Index (VSDI), were calculated utilizing multitemporal Landsat images. Field verification was done for the retrieved parameters needed to calculate the indices i.e., soil moisture content and Land Surface Temperature (LST). Results from various indices were compared to understand the drought pattern in the study area. The VHI revealed that 2014 and 2002 were the most drought-prone year and the drought extent in this region intensified from mild to severe drought. Severe drought was found in northern Lalmonirhat, central Nilphamari, and Thakurgaon, the southern part of Dinajpur, dispersed part of Panchagarh districts and sand bars of the river. It is evident that Thakurgaon, Dinajpur, Gaibandha, and the northern part of Lalmonirhat districts face high agricultural drought risk, Nilphamari, Panchagarh, and Rangpur demonstrate medium risk, and Kurgigram district shows slight agricultural drought risk. The drought severity was mainly triggered out due to the decreasing trend of vegetation identified by the Normalized Difference Vegetation Index (NDVI) and also for the climbing trend of LST. In the year 2018, drought mainly prevailed due to the increased amount of LST mainly in the Nilphamari district. Several regions such as dried river channels, sand bars, and uncultivated land show high drought conditions due to lack of moisture in this region and reduce water flow impeded by the upstream dams. As drought has great impacts on agriculture, it is expected that this satellite-based drought assessment will be beneficial to improve the understanding of drought in the northwestern regions of Bangladesh.

1. Introduction

Drought harms the agricultural, ecological and socio-economic system. Globally, Drought is a common climatic episode that impends the food and water supplies, along with the worldwide economy (Wilhite, 2005; Iglesias et al., 2009). Drought is considered as one of the most expensive and least comprehensive disasters (Zhang et al., 2012). Hence, it has drawn rising attentions from world scientists. Agricultural droughts are characterized by the deficiency of moisture content in soil (Dracup et al. 1980). Agricultural droughts happen once crops become damaged that sometime concurs with the meteorological drought but it depends on the crop stages (Heim et al., 2002). Drought has severe impacts on agriculture, forestry, and fisheries can blow on the economy of a country. Due to inadequate water supply drought events decrease crops and livestock production. Drought also has a great impact on the environment and the influence of drought on the environment is seen as damages to flora and fauna. The social impact of the drought is also observed due to its length of persistence and extremity. In every 2.5

years, an average drought appears in Bangladesh as a common climatic downfall. Historically, 19 droughts events have occurred in Bangladesh between 1960 and 1991 (Adnan, 1993; Hossain, 1990). The principal cause of these droughts is a lesser amount of rainfall and subsequent lower groundwater recharge that play an adverse impact on cropping (Murad & Islam, 2011). Due to drought and associated climate change Bangladesh will be at higher risk in near future (World Bank, 2000).

The North-west region of Bangladesh is one of the most drought-prone areas in Bangladesh. Seasonal drought happens almost on a regular interval in this part of the country (SPARRSO, 2007). Consequently, the crop yields of Bangladesh are severely affected by droughts in this region. Rangpur division, where the majority of the population dependent on agriculture, is affected severely by the occurrence of agricultural drought. Agricultural drought causes despair in the population and livestock in the whole region. Mishra & Singh (2010) defined agricultural drought as a period with decreasing moisture in the soil and resultant crop failure along with other factors i.e., precipitation, evapotranspiration, plant characteristics, growth stages. However, the present research deals with the assessment of agricultural droughts in the study

* Corresponding author.

E-mail address: yousuf.geo@du.ac.bd (Md.Y. Gazi).

Table 1

Satellite images with their acquisition date, path, raw and spatial resolution.

| Sensor Platform | Acquisition Date | Path | Raw | Scene ID | Cloud Cover (%) | Spatial Resolution |
|--------------------|------------------|------|-----|-----------------------|-----------------|--------------------|
| Landsat TM | 29.10.1990 | 138 | 42 | LT51380421990302BKT00 | 0 | 30 m |
| | 29.10.1990 | 138 | 43 | LT51380431990302BKT00 | 2 | |
| | 20.10.1990 | 139 | 42 | LT51390421990293BKT00 | 1 | |
| Landsat ETM+ | 23.11.2002 | 138 | 42 | LE71380422002327SGS00 | 0 | 30 m |
| | 23.11.2002 | 138 | 43 | LE71380432002327SGS00 | 0 | |
| | 16.12.2002 | 139 | 42 | LE71390422002350SGS01 | 2 | |
| Landsat (OLI/TIRS) | 02.12.2014 | 138 | 42 | LC81380422014336LGN01 | 1 | 30 m |
| | 02.12.2014 | 138 | 43 | LC81380432014336LGN01 | 0 | |
| | 23.11.2014 | 139 | 42 | LC81390422014327LGN01 | 0 | |
| | 11.11.2018 | 138 | 42 | LC81380422018315LGN00 | 2 | |
| | 11.11.2018 | 138 | 43 | LC81380432018315LGN00 | 1 | |
| | 02.11.2018 | 139 | 42 | LC81390422018306LGN00 | 0 | |

area mainly based on the soil moisture content using satellite remote sensing and field-based observations.

It is possible to reduce the impacts of drought by satellite image-based spatial monitoring of drought regularly. In recent years, satellite-based agricultural drought monitoring has become more popular and is widely used within various regions around the world (Zhang et al., 2014). Remote sensing and GIS have been extensively utilized over the past decades to monitor environmental problems including drought (Caccamo et al., 2011; Rhee et al., 2010; Mladenova et al., 2014; Zhang & Jia, 2013; Choi & Hur, 2012; Mahyou et al., 2010; Abdrabbo et al., 2012). Various remote sensing-based indexes such as NDVI, LST, VCI, TCI, VHI, TVDI, VSIDI, and Crop Moisture Index (CMI) have been popularly applied to assess the agricultural droughts concerning plant growth and cultivation (Han et al., 2010; Wilhite, 2005; Tucker et al., 1983). Ghaleb et al. (2015) carried out a study in Lebanon to monitor agricultural drought using VCI, TCI, and VHI. A similar study has also been done in Indonesia (Sholihah et al., 2016). Kogan (1995) conducted a study using satellite image (AVHRR) based on VCI/TCI application in various ecological environments of the United States. Sruthi & Aslam (2015) conducted a study on agricultural drought monitoring with the help of geospatial techniques in the Raichur District, of Karnataka (India) using MODIS data. In the Indian sub-continent, drought has been also studied extensively using GIS and Remote Sensing tools to monitor the Spatio-temporal pattern of agricultural drought (Aswathi et al., 2018; Vaani & prochelvan, 2018; Dhawale & Paul, 2018; Baniya et al., 2019; Padhe et al., 2017). Some recent works focused on the assessment of agricultural drought throughout the world (Dai et al., 2020; (Han et al., 2021); Mladenova et al., 2020). Several works used remote sensing and GIS techniques to drought in different parts of the world (Yoon et al., 2020; Almamalachy et al., 2020; Liu et al., 2020; Sandeep et al., 2021). Recently, soil moisture content has been used by some research to evaluate agricultural droughts (Souza et al. 2021; Zhou et al., 2021). Very few works were conducted in the Northwest region of Bangladesh based on GIS and Remote sensing techniques (Murad & Islam, 2011; Neupane et al., 2014). These works are only based on the simple distribution of rainfall patterns in the Northwest region of Bangladesh. There has been not as much research on the comprehensive drought index concerning soil moisture content, vegetation health condition, and LST of the region. Therefore, in this study, Landsat satellite data were utilized to retrieve the drought indices for different years.

To attain sustainable growth in agricultural productivity and improve the livelihoods of the drought-prone people, agricultural drought monitoring is the most viable way for mitigating the problems on both local and regional scales. Since drought possesses an adverse impact on environmental sustainability, research in this arena is very crucial to understand the characteristics, occurrence, and impacts of drought on the local and regional scale. The present research was attempted to monitor the agricultural drought effectively with several drought indices for sustainable farming and land-use planning in the study area.

The prime objective of this study is to identify and monitor agricultural drought in the northwestern region of Bangladesh using multispectral satellite images. Assessment of several drought indices, the relationship among these indices, and calculation of drought area extent, duration, intensity, and severity of the drought is the prime concern. The study will enable us to make a proper plan for irrigation practice in drought vulnerable areas and will provide prior knowledge of challenges during cultivation in this region.

2. Materials and methods

2.1. Study area

The northwest region of Bangladesh consists of 8 districts namely Rangpur, Panchagarh, Nilphamari, Lalmonirhat, Nilphamari, Kurigram, Thakurgaon, Dinajpur, and Gaibandha (BBS, 2011) (Fig. 1). The region occupies an overall area of 16,184.99 km² with a population density of around 980 per sq. Km (Murad & Islam, 2011). Two third of people live from agricultural activities in this region. Paddy is the main crop in this region which is grown at a different time of the year. Other crops in descending order of importance are wheat, jute, oilseeds, sugarcane, pulses, vegetables, and spices.

The NW region has an extreme tropical monsoon climate characterized by two main seasons, a rainy season from June to October and a dry season from November- March. Average annual rainfall ranges from less than 1500 mm to 3000 mm with a regional average of about 1583 mm (Murad & Islam, 2011). Temperature variations are more pronounced in the N-W region of Bangladesh due to subtropical location (Islam & Miah, 1981). Maximum temperature ranges from 36°C in April/May, occasionally exceed 38°C to 25°C in January. Minimum temperature varies from 20°C in August to 10 to 20°C in January.

The area is segmented into three physiographic divisions i.e., Himalayan Piedmont Plain, Tista Flood-Plain, and Barind Tract. Due to extreme monsoon climate and different soil composition, the vegetation shows significant variation ranging from grassland to deciduous, mixed to evergreen. Rice is the main crop in this region (Reiman, 1993). The major rivers which pass through the study area are the Brahmaputra, Jamuna, Punarbhaba, Karatoya, Atrai, Tista, mahananda, Dharla, Ghaghat, Dhepa, and Dhudkumor.

2.2. Used datasets

This study used multispectral satellite images (Landsat TM, Landsat ETM+, and Landsat OLI/TIRS) from 1990 to 2018 (<https://earthexplorer.usgs.gov/>) and field data (Table 1). The images are radiometrically and atmospherically corrected. Two main geospatial software used in this study for data processing and analysis such as Erdas Imagine 2014 and ArcGIS 10.3. Around 80 ground measurements were taken using a “Eurolab ST92698 Multi Thermometer” to validate the LST data obtained from the image. This meter can

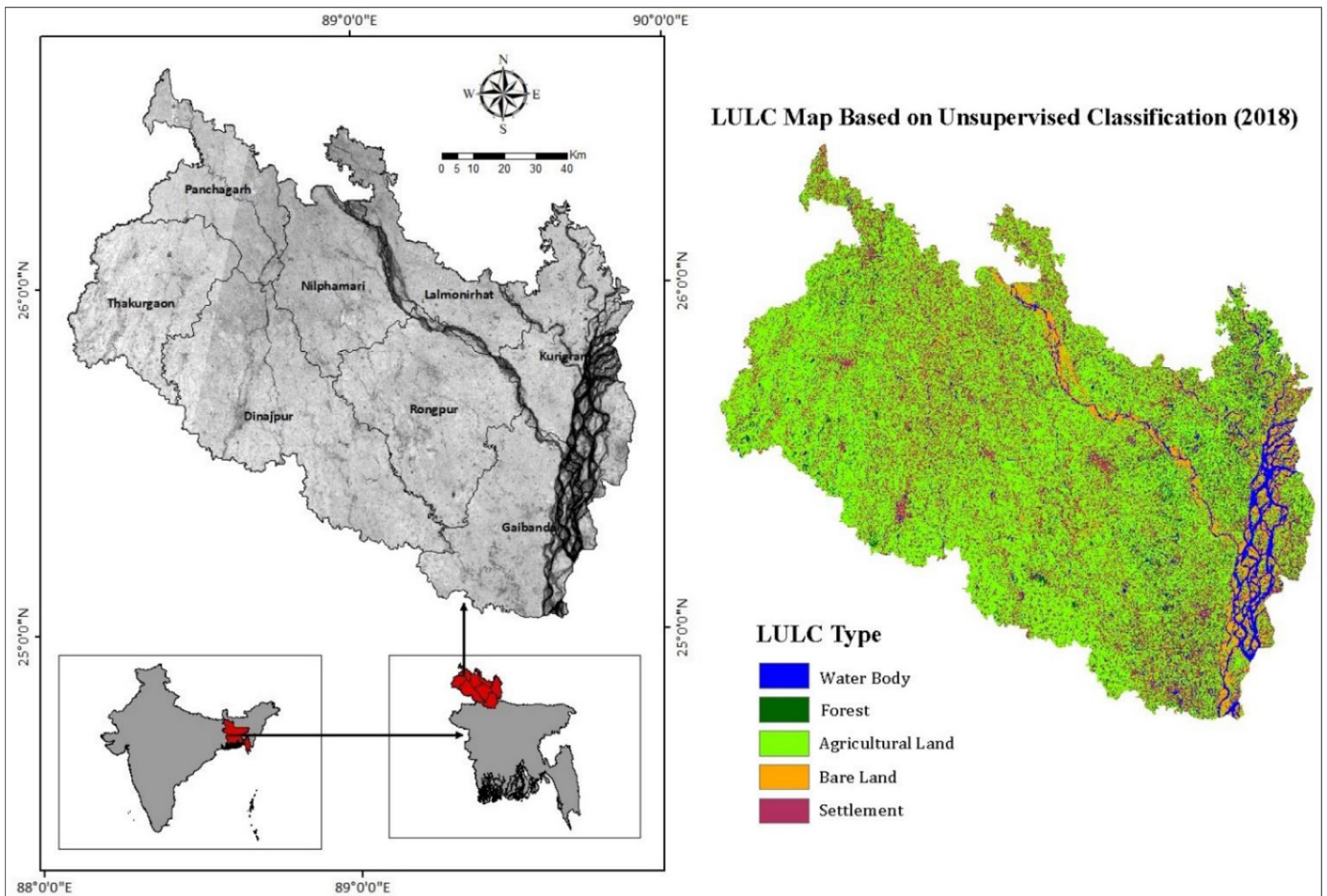


Fig. 1. Location of the study area, northwest region, Bangladesh including landuse-landcover information (2018). The background is Landsat 8 satellite image (band 4) 2018.

measure in the range of -50°C to $+300^{\circ}\text{C}$ or -58°F to $+572^{\circ}\text{F}$ by its stainless-steel probe including 1-meter wire code with an accuracy level $\pm 1^{\circ}\text{C}$ up to 200°C . For measuring temperature, the probe of the thermometer has been inserted into the ground and penetrated at a depth of about 1.2 to 2 cm. To read data more accurately, the meter kept for 1 min for stabilization. In the same sampling points, soil moisture was also recorded by the PMS-714 handheld soil moisture meter. The measurements were taken using the conductive principal, then converts the reading to the % moisture content. It has a stainless-steel probe with the length of 20 cm. It can measure in a range of 0 to 50% moisture content. This instrument has an accuracy level $\pm (5\% \text{ F.S.} + 5 \text{ d})$ with 0.1 % resolution. Moisture sensing head of the soil moisture meter was inserted around 5-8cm into the ground to read moisture data in the study area.

2.3. Data analysis

In this study, agricultural drought was monitored through multiple indices such as VHI, TVDI, VSDI. VHI is based on the moisture condition of vegetation (VCI) and thermal condition of vegetation (TCI). VCI is based on the NDVI and TCI on LST. Another two indices, TVDI and VSDI were computed based on the LST and NDVI and the difference between moisture-sensitive bands (SWIR and red) and a moisture reference band (blue) respectively (Fig. 2).

NDVI was a pre-requisite for the estimation of VCI. The NDVI was calculated from these specific bands as follows ([Landsat 8 data user handbook, 2015](#)):

$$NDVI = (NIR - RED)/(NIR + RED) \quad (1)$$

Here, NIR and RED stand for the spectral reflectance attained in the near-infrared regions and red (visible) respectively.

To calculate Land Surface Temperature (LST), several parameters have to be retrieved. The steps involved, conversion of DN values to radiance values. Then, Land surface Brightness Temperature (LST_B) calculated using temperature constants to put as input in the final equation. Vegetation (P_V) coverage calculated from NDVI and Land surface Emissivity from Vegetation (P_V) coverage. Finally, the outputs are used to retrieve true skin land surface temperature (LST) ([Stathopoulou, & Cartalis, 2007](#)).

$$LST = (BT/(1 + (\lambda * BT/\rho) * Ln(\epsilon))) - 273.15 \quad (2)$$

Where LST = Land Surface Temperature in Celsius ($^{\circ}\text{C}$)

BT = Sensor Brightness Temperature in ($^{\circ}\text{C}$)

λ = Wavelength of Thermal Band of various Landsat Satellite

ϵ = Emissivity of the Land Surface

ρ = ($h \times (c/\sigma)$), which is equal to $1.438 \times 10^{-2} \text{ mK}$

In which, σ is the Boltzmann constant ($1.380649 \times 10^{-23} \text{ J/K}$), h is Plank's constant ($6.62607015 \times 10^{-34} \text{ J.s}$ and c is the velocity of light ($3 \times 10^8 \text{ m/s}$).

Kogan (1995) established the vegetation condition index (VCI) to monitor local changes in ecosystem productivity. The purpose of VCI estimation was a prerequisite to retrieve another drought index VHI. The NDVI and VCI have been accepted universally for recognizing agricultural drought in diverse regions with changing ecological conditions ([Seiler et al. 2000; Ji and Peters 2003](#)). Kogan (2004) provided the following formula for the Vegetation Condition Index (VCI):

$$VCI = 100 * (NDVI - NDVI_{min}) / (NDVI_{max} - NDVI_{min}) \quad (3)$$

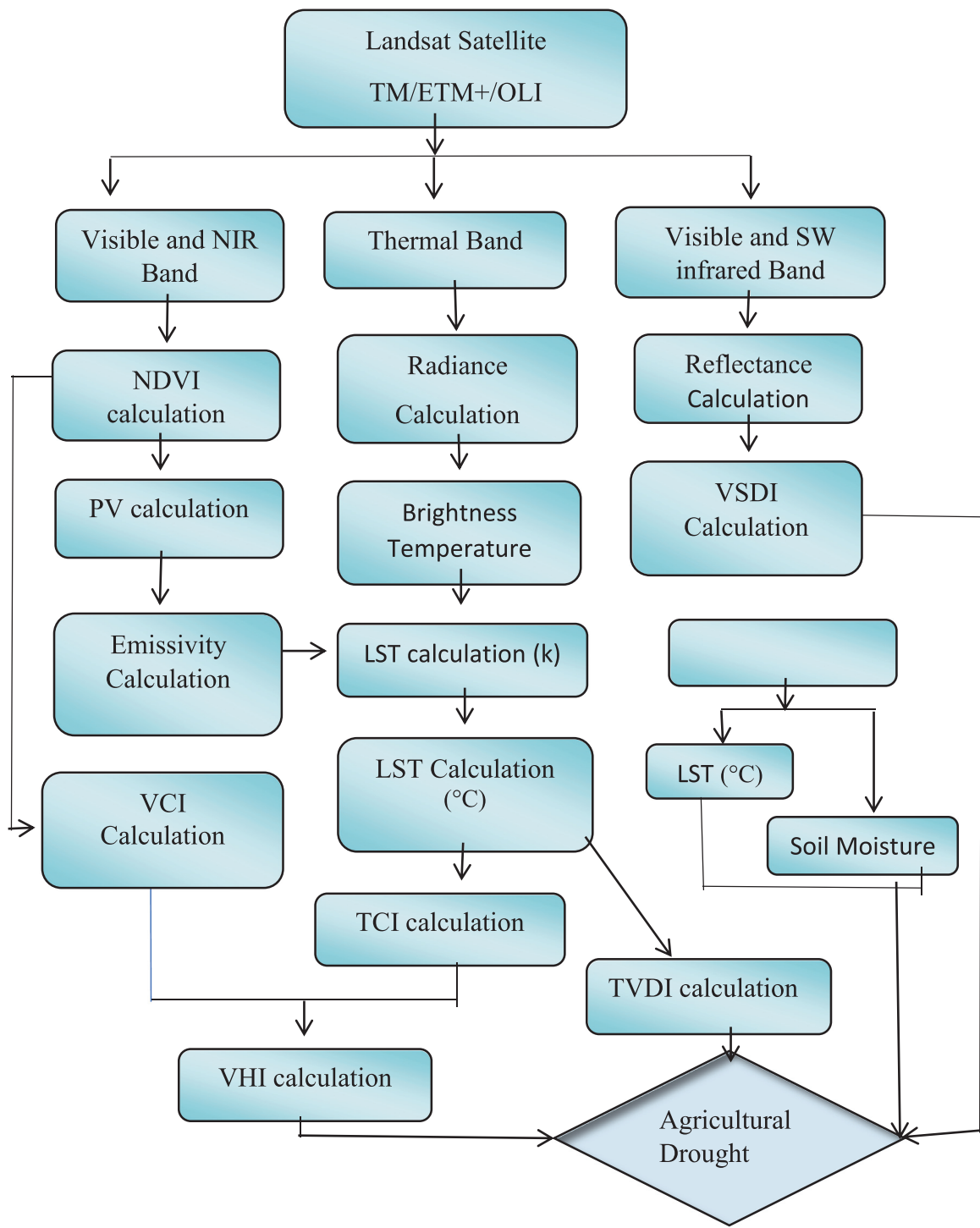


Fig. 2. Methodology flowchart showing the work steps involved in this study.

Where NDVI = Smoothed yearly NDVI value

$NDVI_{min}$ = Multiyear minimum NDVI value

$NDVI_{max}$ = Multiyear maximum NDVI value

From extremely unfavorable to optimal VCI changes from 0 to 100 corresponding to changes in vegetation condition (Kogan, 1995).

The TCI calculation is somewhat similar to VCI reflecting the vegetation's response to temperature (i.e., more extreme the drought shows for the higher temperature). Thus, the TCI formula was improved as the following equation:

$$TCI = 100 * (LST_{max} - LST / LST_{max} - LST_{min}) \quad (4)$$

Where LST = LST value for the current month

LST_{max} & LST_{min} = Multilayer maximum and minimum temperature consecutively.

The VHI symbolizes vegetation health because stressed conditions are connected to a higher temperature and lower than normal NDVI (Kogan, 1997). This index integrates TCI and VCI linking the soil moisture and thermal stress to provide total vegetation health condition. The equation for VHI is given by Kogan (1997).

$$VHI = \alpha VCI + (1 - \alpha) TCI \quad (5)$$

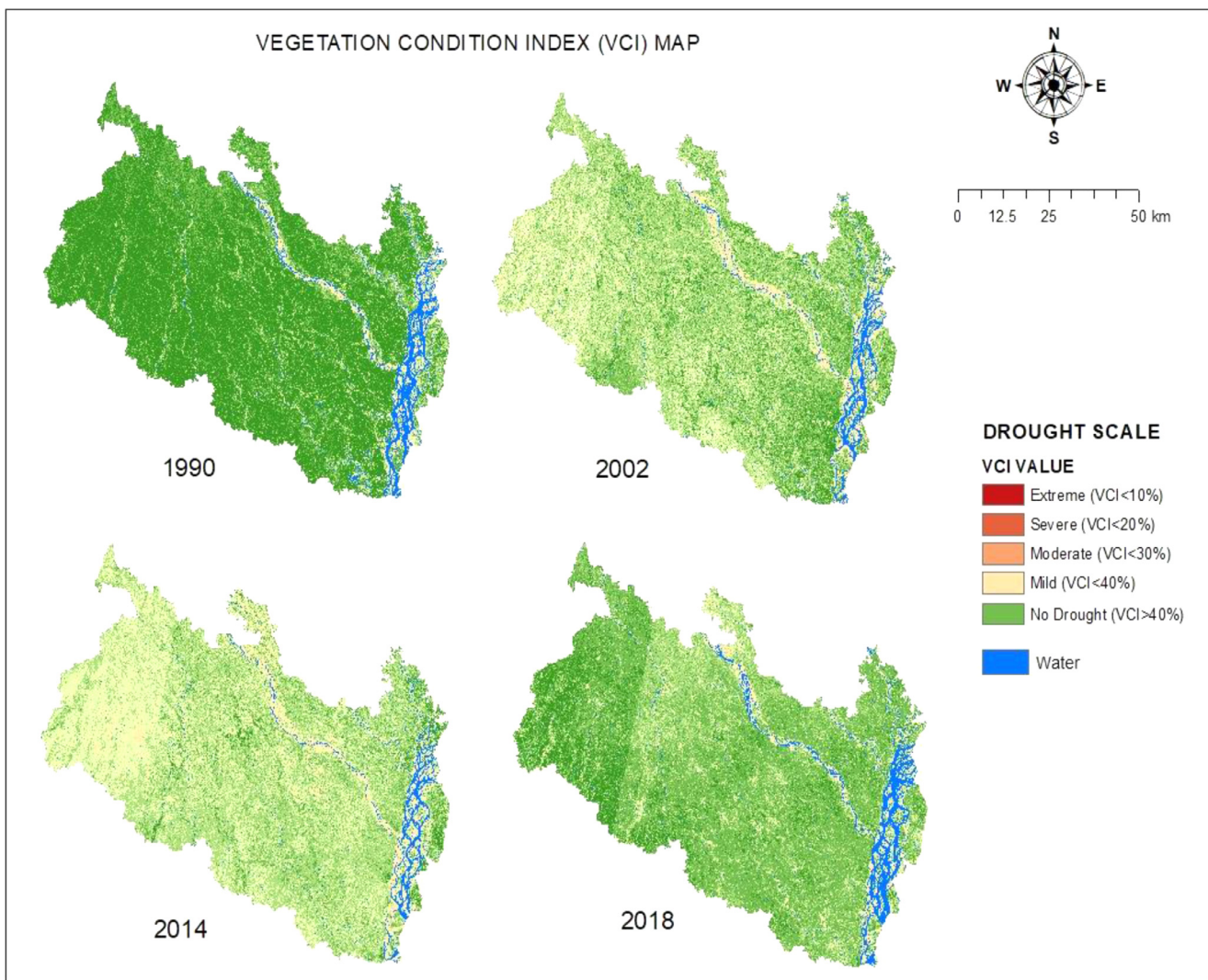


Fig. 3. Spatial distribution of drought based on the VCI.

Table 2
Drought classification in terms of VCI, TCI, VHI Value (Ghaleb et al., 2015, Kogan, 1995).

| Drought | Value |
|------------|-------|
| Extreme | <10 |
| Severe | <20 |
| Moderate | <30 |
| Mild | <40 |
| No Drought | >40 |

Table 3
Classification of soil moisture based on TVDI Value (Han et al. 2010).

| Soil Moisture | TVDI Value |
|---------------|------------------------|
| Very Wet Soil | ($0 < TVDI < 0.1$) |
| Wet Soil | ($0.1 < TVDI < 0.4$) |
| Normal Soil | ($0.4 < TVDI < 0.6$) |
| Dry Soil | ($0.6 < TVDI < 0.9$) |
| Very Dry Soil | ($0.9 < TVDI < 1$) |

Where α is a parameter that measures the influence of individual components on the total vegetation health. The value of α is equaled to 0.5 (Kogan, 2001; Rojas et al., 2011). Drought classification in terms of VCI, TCI, and VHI value is given below (Ghaleb et al., 2015, Kogan, 1995) (Table 2).

Temperature Vegetation Dryness Index (TVDI) was proposed by Sandholt et al. (2002) to assess drought severity depending on LST and NDVI. It quantifies soil moisture content (Table 3).

$$TVDI = LST - LST_{min}/LST_{max} - LST_{min} \quad (6)$$

Where $LST_{max} = a1 + b1 \times NDVI$, $LST_{min} = a2 + b2 \times NDVI$

Where LST stands for observed skin surface temperature ($^{\circ}\text{C}$). LST_{max} is the maximum surface temperature for a specified NDVI and $a1$ and

Table 4
Drought classification scheme of VSDI (Zhang et al., 2013).

| Drought Type | VSDI Range |
|---------------------|-------------------------|
| Normal | $VSDI \geq 0.75$ |
| Abnormally dry | $0.71 \leq VSDI < 0.75$ |
| Moderate drought | $0.68 \leq VSDI < 0.71$ |
| Severe drought | $0.64 \leq VSDI < 0.68$ |
| Extreme drought | $0.61 \leq VSDI < 0.64$ |
| Exceptional drought | $VSDI < 0.61$ |

$b1$ express the dry edge as a linear fit to the data; $a2$ and $b2$ outline the wet edge.

Table 5

Summary results of VCI based drought in the years 1990, 2002, 2014, and 2018.

| Used Index | Drought Severity Class | 1990 Area (km ²) | Area (%) | 2002 Area (km ²) | Area (%) | 2014 Area (km ²) | Area (%) | 2018 Area (km ²) | Area (%) |
|------------|------------------------|------------------------------|----------|------------------------------|----------|------------------------------|----------|------------------------------|----------|
| VCI | Extreme | 0.00 | 0.00 | 0.20 | 0.00 | 0.40 | 0.00 | 0.00 | 0.00 |
| | Severe | 0.50 | 0.00 | 1.50 | 0.01 | 3.50 | 0.02 | 0.60 | 0.00 |
| | Moderate | 171.05 | 1.06 | 457.59 | 2.83 | 313.99 | 1.94 | 180.64 | 1.12 |
| | Mild | 96.51 | 0.60 | 733.40 | 4.53 | 1152.26 | 7.12 | 576.62 | 3.56 |
| | No Drought | 15916.00 | 98.34 | 14992.30 | 92.63 | 14714.00 | 90.91 | 15427.13 | 95.32 |

Table 6

Summary outcomes of TCI based drought in the years 1990, 2002, 2014, and 2018.

| Used Index | Drought Severity Class | 1990 Area (km ²) | Area (%) | 2002 Area (km ²) | Area (%) | 2014 Area (km ²) | Area (%) | 2018 Area (km ²) | Area (%) |
|------------|------------------------|------------------------------|----------|------------------------------|----------|------------------------------|----------|------------------------------|----------|
| TCI | Extreme | 19.23 | 0.12 | 225.7 | 1.39 | 421.7 | 2.61 | 154.39 | 0.95 |
| | Severe | 111.30 | 0.69 | 744.83 | 4.60 | 2856.02 | 17.65 | 524.21 | 3.24 |
| | Moderate | 2464.21 | 15.23 | 6057.24 | 37.43 | 12566.35 | 77.64 | 6200.29 | 38.31 |
| | Mild | 8171.28 | 50.49 | 7706.61 | 47.62 | 339.37 | 2.10 | 7952 | 49.13 |
| | No Drought | 5418.97 | 33.48 | 1450.61 | 8.96 | 1.55 | 0.01 | 1354.1 | 8.37 |

Table 7

Summary outputs of VHI based drought in the years 1990, 2002, 2014, and 2018.

| Used Index | Drought Severity Class | 1990 Area (km ²) | Area (%) | 2002 Area (km ²) | Area (%) | 2014 Area (km ²) | Area (%) | 2018 Area (km ²) | Area (%) |
|------------|------------------------|------------------------------|----------|------------------------------|----------|------------------------------|----------|------------------------------|----------|
| VHI | Extreme | 0 | 0.00 | 0 | 0.00 | 0.2 | 0.00 | 0.0729 | 0.00 |
| | Severe | 0 | 0.00 | 0.1 | 0.00 | 716.17 | 4.42 | 0 | 0.00 |
| | Moderate | 1134.38 | 7.01 | 1747.42 | 10.80 | 6895.44 | 42.60 | 1359.69 | 8.40 |
| | Mild | 1729.19 | 10.68 | 9843.1 | 60.82 | 5610.2 | 34.66 | 5079.49 | 31.38 |
| | No Drought | 13321.42 | 82.31 | 4593.6 | 28.38 | 2962.98 | 18.31 | 9745.69 | 60.21 |

Drought Area Trend from VCI value

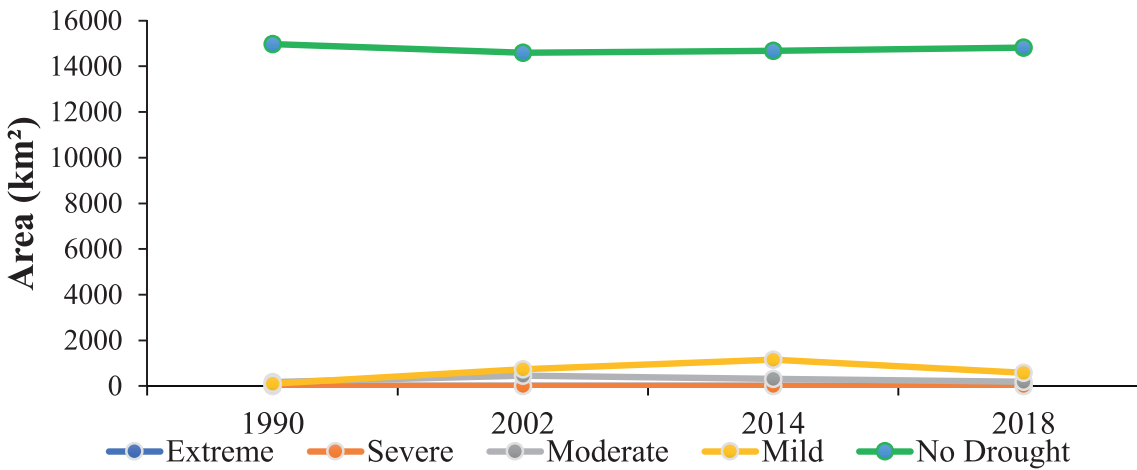


Fig. 4. Comparison of drought based on VCI in 1990, 2002, 2014 and 2018.

The visible and shortwave infrared drought index (VSDI), is established for assessing both soil and vegetation moisture content employing optical spectral bands (Table 4). The formula for calculating VSDI is (Zhang et al, 2013):

$$VSDI = 1 - [(\rho_{SWIR} - \rho_{blue}) + (\rho_{red} - \rho_{blue})] \quad (7)$$

Where, ρ signifies the reflectance of shortwave infrared (SWIR), red and blue channels, consecutively.

3. Results

Agricultural drought in the study area has been assessed by the indices (VCI, TCI, VHI, TVDI, VSDI) to monitor the drought severity from 1990 to 2018.

3.1. Vegetation Condition Index (VCI)

Drought has been classified into five classes based on the VCI values such as extreme, severe, moderate, mild, and no drought areas. The result of the VCI thematic map for the year 1990 shows almost no extreme and severe drought. Moderate drought covered an area of 171.05 km² which is only 1.06 % of the total study area. Sand Bar of the Brahmaputra, Tista, and Dharla Rivers located in the eastern and north-eastern corner of the study area represents moderate drought conditions. Mild drought risk area prevails only 0.60 % of the total study area (Table 5). A significant amount of vegetation has been lost and bare land has been increased in 2002. Only a small part of the Gaibandha district near the Brahmaputra River shows healthy vegetation cover. About 457.59 km² and 733.40 km² areas represent moderate and mild drought respectively which are 2.83% and 4.53% of the total geographic area in 2002. The western part of the Thakurgaon district and the sand bar of the Tista

TEMPERATURE CONDITION INDEX (TCI) MAP

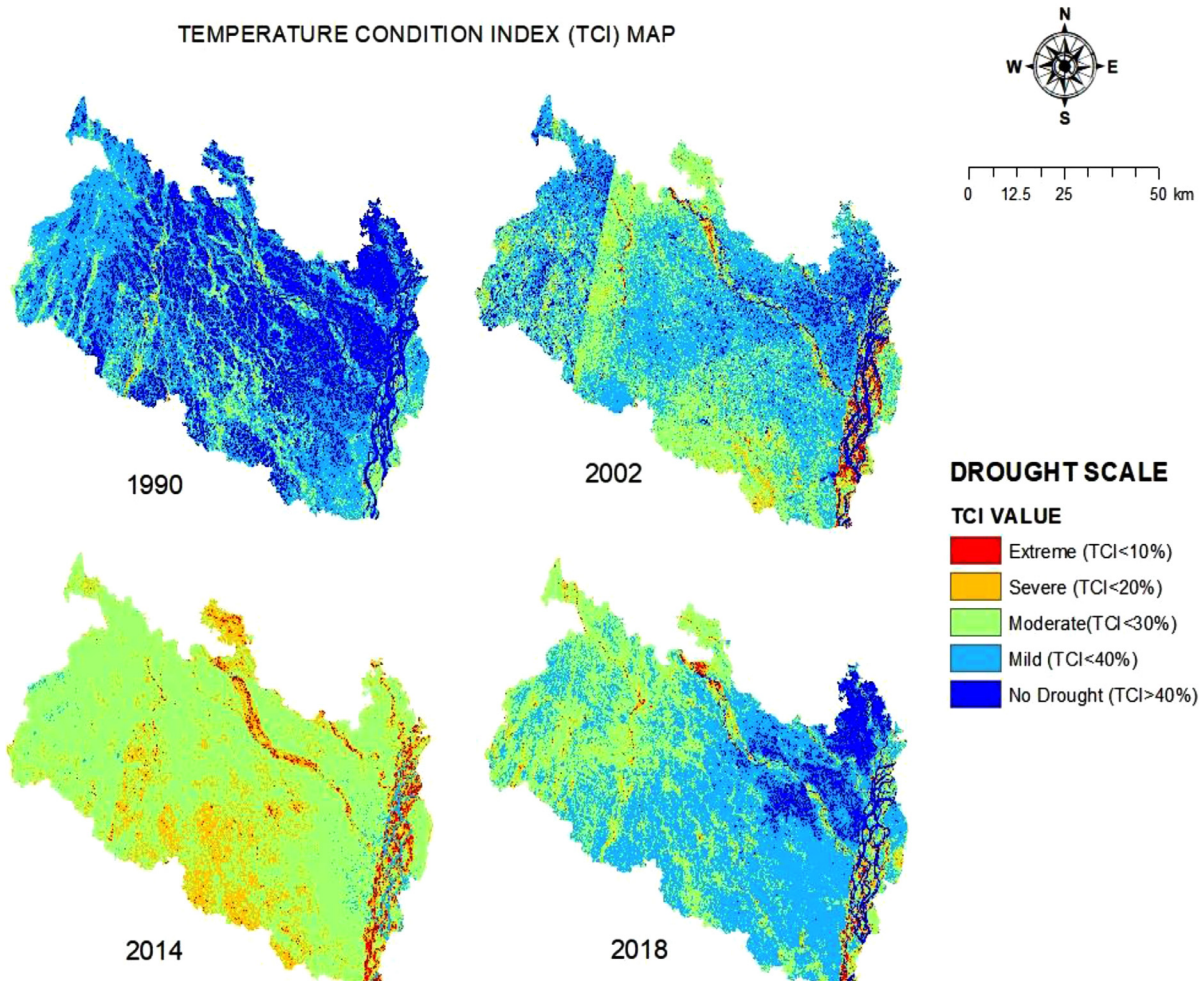


Fig. 5. TCI based drought extent for the years 1990, 2002, 2014, and 2018.

Drought Area Trend from TCI Value

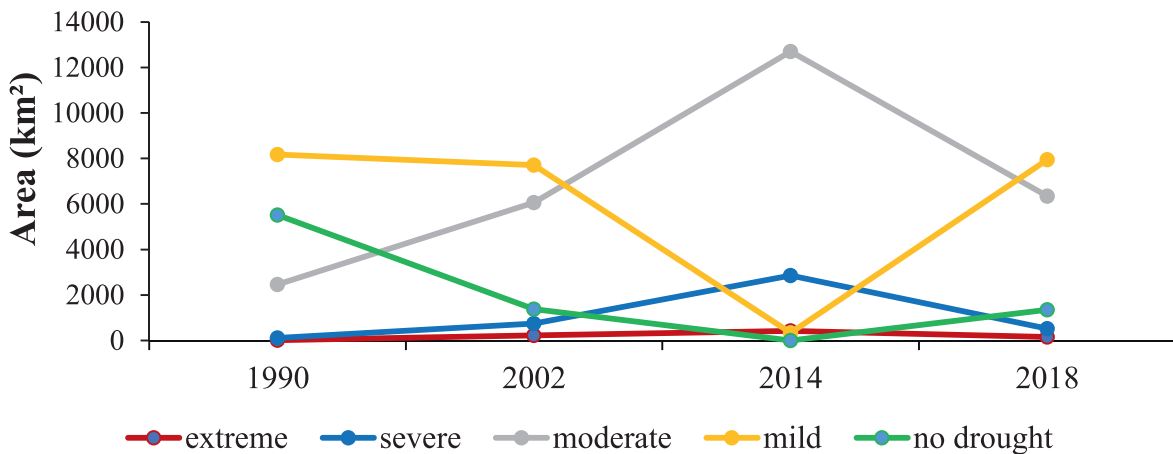


Fig. 6. Drought severity trends based on TCI from 1990 to 2018.

River areas represent moderate drought. In 2014, 313.99 km² areas have been identified as moderate drought and these are 1.94% of the study area. The central part of the Thakurgaon district, the northern part of the Lalmonirhat district, and the river sand bar were identified as moderate drought conditions (Fig. 3). The study reveals that mild drought occupies about 1152.2 km² area which is 7.12% of the study area. In 2018,

about 1.12% of the total study area shows moderate drought. Some areas near the Tista river of Lalmonirhat districts displayed moderate drought situations. Saidpur of Rangpur, several parts of Nilphamari, North-East corner of Lalmonirhat district revealed mild drought risk (3.56%).

The VCI based study shows that the year 2014 is comparatively more drought-prone than other study years. The result indicates that the mild

VEGETATION HEALTH INDEX (VHI) MAP

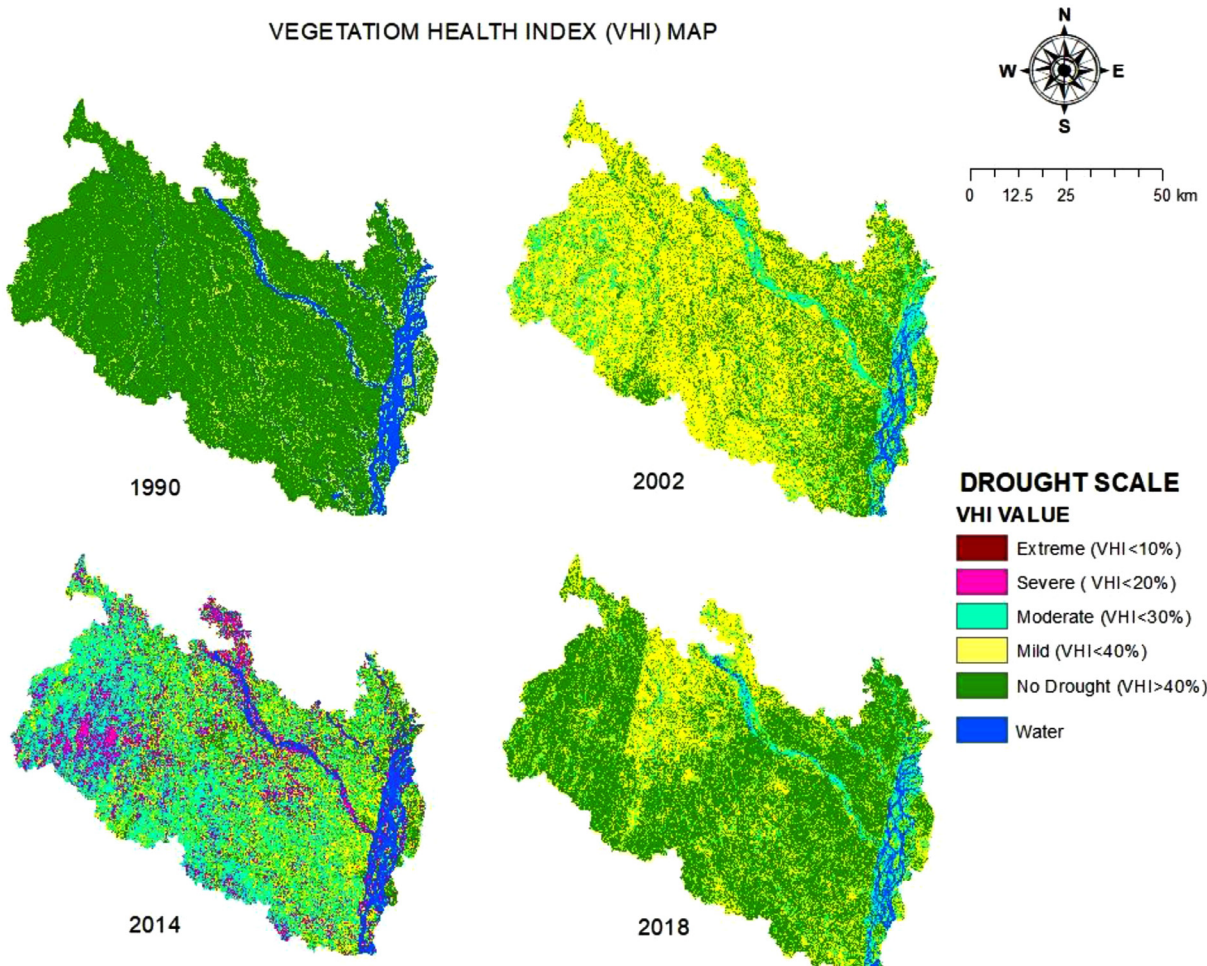


Fig. 7. Thematic spatial distribution of VHI based drought in the years 1990, 2002, 2014, and 2018.

Drought Area Trend from VHI Value

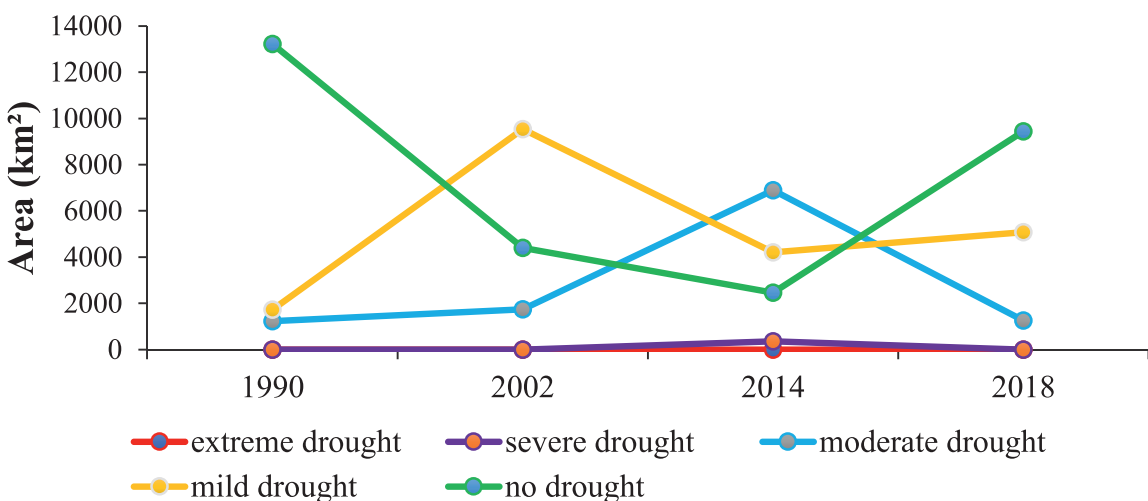


Fig. 8. Trends of drought extent based on VHI for the years 1990, 2002, 2014, and 2018.

drought area is at the peak in 2014 (7.12%) and is at the bottom in the year of 1990 (0.60%) among the four years (Fig. 4). The second highest drought area was found in 2002 about 2.83% of the total area as moderate drought. Among the four years of this study, both the year 2014 and 2002 were detected with moderate to mild drought areas. On the other hand, most of the study area was found as no drought in the years 1990 and 2018.

3.2. Temperature Condition Index (TCI)

Drought has been classified into five classes based on the TCI values such as extreme, severe, moderate, mild, and no drought areas based on TCI. In 1990, extreme drought covers 19.23 km² areas which are 0.12% of the total study area (Table 6). River sand bar (Atrai, Karatoya, Tista, Dharla, and Brahmaputra) characterize extreme drought sever-

TEMPERATURE VEGETATION DRYNESS INDEX (TVDI) MAP

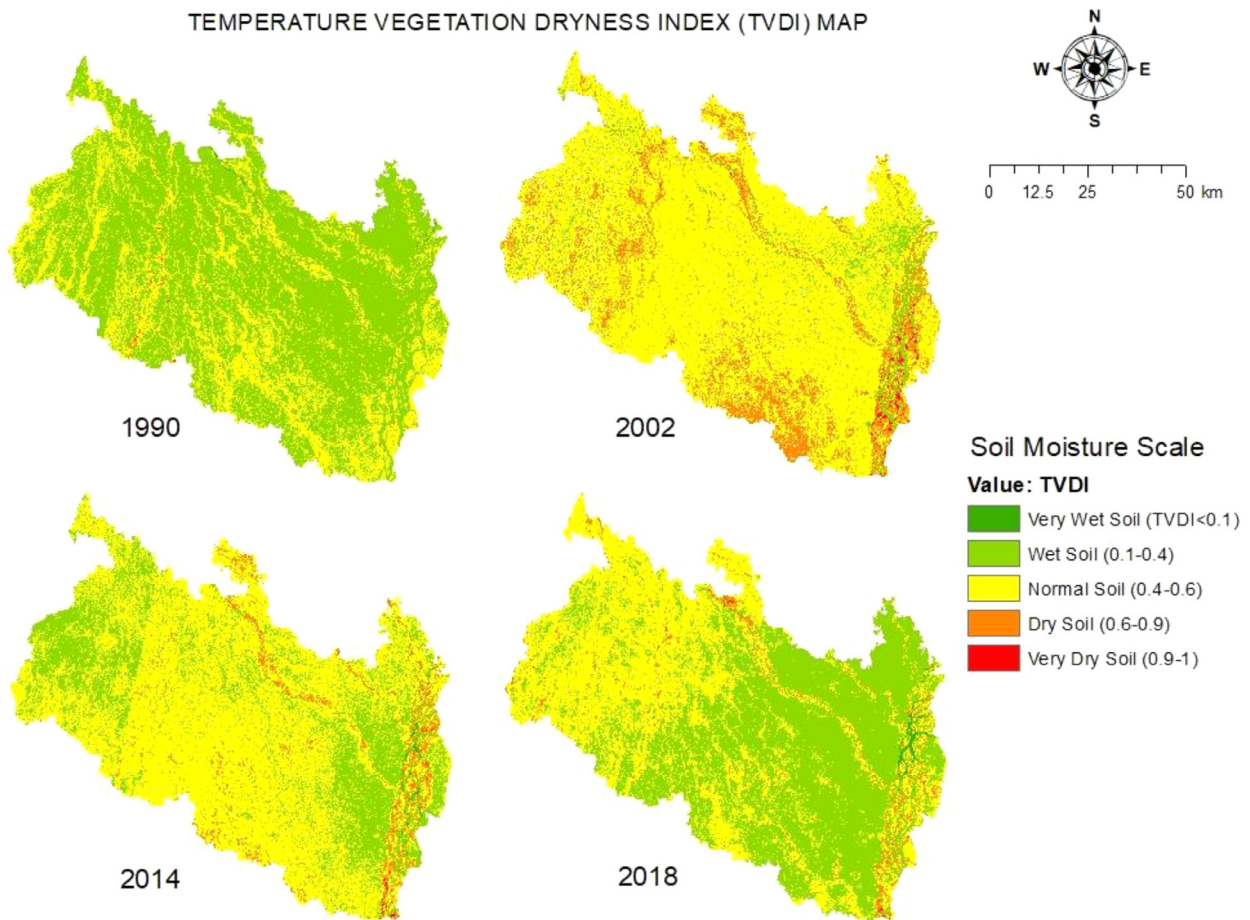


Fig. 9. Spatial extent of drought based on the TVDI.

ity in this year. The study identifies 111.30 km² area as severe drought which is 0.69% of the total area. Sand bar of the various river showed severe drought conditions. Moderate drought encompasses 2464.21 km² area which is 15.23% of the total area. Eastern and southwest corner of Thakurgaon districts, a large area of Birampur Upazila, the middle part of Nilphamari districts, and several areas near Brahmaputra river of Gaibandha districts notify moderate drought class (Fig. 5). About 8171.28 km² area showed mild drought which is 33.48 % of the study area. In 2002, 1.39% of the total area shows extreme drought class. Severe drought indicates 4.60% of the total area which comprises the south-east corner of Gaibandha, scattered part of Thakurgaon and Dinajpur, and river sand bar (Brahmaputra and Tista). The Southwest corner of Gaibandha, the lower part of Birmpur, Eastern Panchagarh, Western Dinajpur, and Northern Lalmonirhat displays moderate drought. Mild drought covered a large area of Rangpur, Kurigram, Lalmonirhat, Gaibandha, Nilphamari, and Dinajpur districts.

In 2014, River (Brahmaputra, Dharla, Tista) sand bar was noted as an extreme drought (2.61%) condition. A large part of Dinajpur, Northern Lalmonirhat, and few parts of North-East Panchagarh was identified as severe drought (17.65%). Very few areas in the North-West corner of Dinajpur represented mild drought (2.10%) conditions. In 2018, River (Brahmaputra, Dharla, Tista, Karatoya) sand bar indicates extreme drought (0.95%) condition (Fig. 6). Eastern Kurigram near Brahmaputra River and some parts of the study area exhibits severe drought (3.24%). A large area of South Eastern and Central Districts of the study area shows mild drought (49.13%) state.

Among all of the years, the maximum extreme drought area was found in the year 2014 and a minimum in 1990. The severe drought is also highest in 2014 and lowest in 1990. Mild drought area was almost

similar among the years of 1990, 2002, and 2018. No drought area was maximum in 1990 and a minimum in the year 2014 but it was almost similar in the year 2002 and 2018.

3.3. Vegetation Health Index (VHI)

In 1990, extreme and severe drought were absent. River sand bar indicated moderate drought (7.01%). Some parts of Dinajpur, Gaibandha, Nilphamari, Rangpur, and Kurigram districts display mild drought (10.68%) (Table 7). Extreme and severe drought is also absent in 2002. River sand bars (Brahmaputra, Dharla, Tista, Karatoya) and a large area of Thakurgaon experiences moderate drought (10.80%). Northern, Southern, Western, and central districts of the study area cover a huge extent of mild drought (60.82%). Extreme drought is absent in 2014 but severe drought covers (4.42%) northern Lalmonirhat, central Nilphamari and Thakurgaon, Southern part of Dinajpur, a small part of Panchagarh, and river sand bars. Moderate drought (42.60%) encloses the South-Western districts (Dinajpur and Thakurgaon) of the study area whereas Mild drought (31.38%) areas were prominent near the Brahmaputra river of Gaibandha and Kurigram districts in 2014 (Fig. 7). River (Brahmaputra, Dharla, Tista, Karatoya) sand bar, few areas of Dinajpur, Gaibandha, Thakurgaon, and Nilphamari districts displays moderate drought (8.40%) state in 2018.

The year 2014 is reported as the most drought-prone among all of the years. Extreme drought condition was absent in all of the year. A severe drought condition was found only in the year 2014. Each year shows moderate drought conditions among, which 2014 has been identified with maximum extent (Fig. 8). Mild drought cover was prominent in

Soil Moisture Trend from TVDI Value

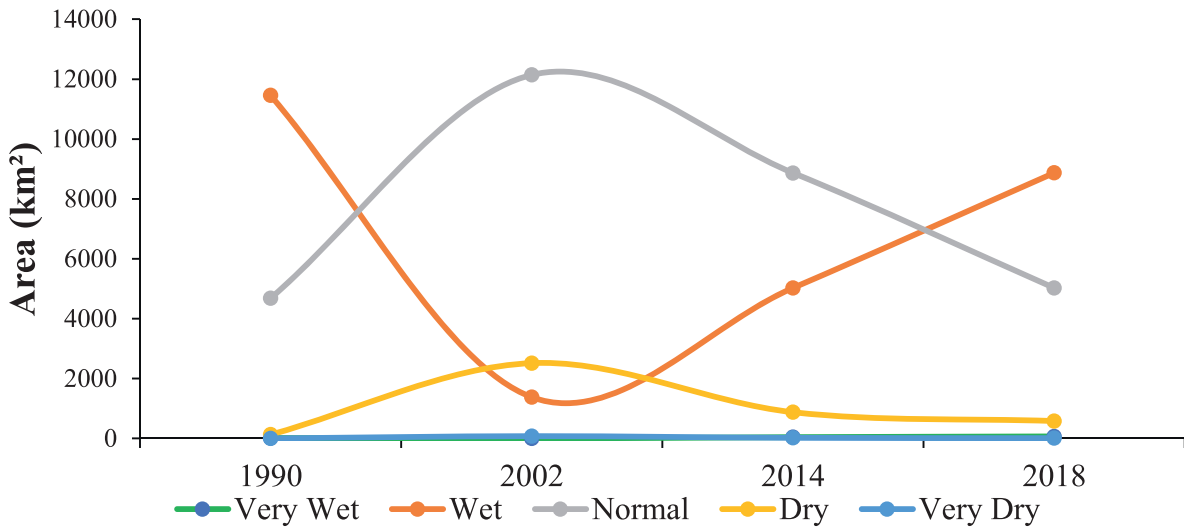


Fig. 10. Drought severity trend based on TVDI.

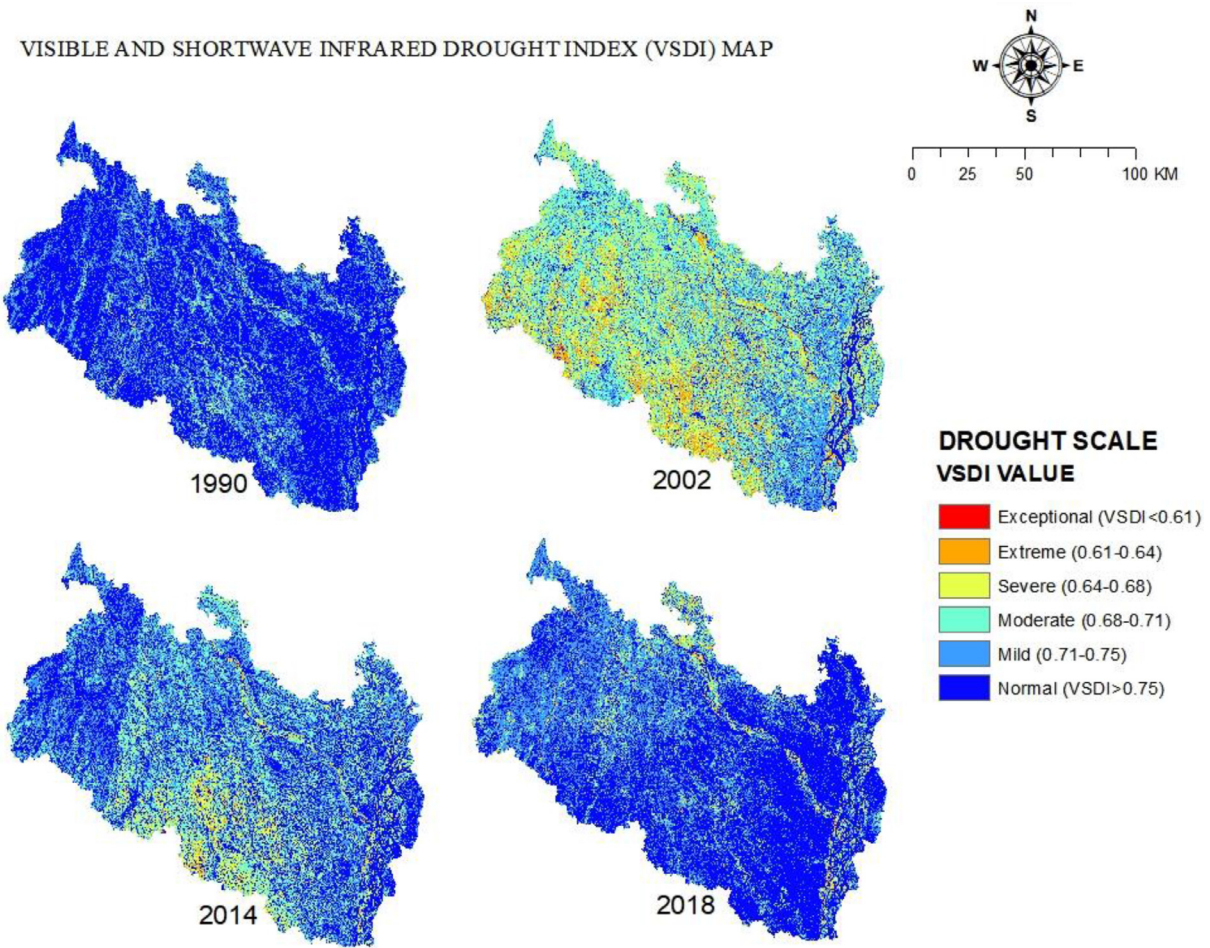


Fig. 11. Spatial distribution of drought thematic classes based on the VSDI.

Drought Area from VSDI Value

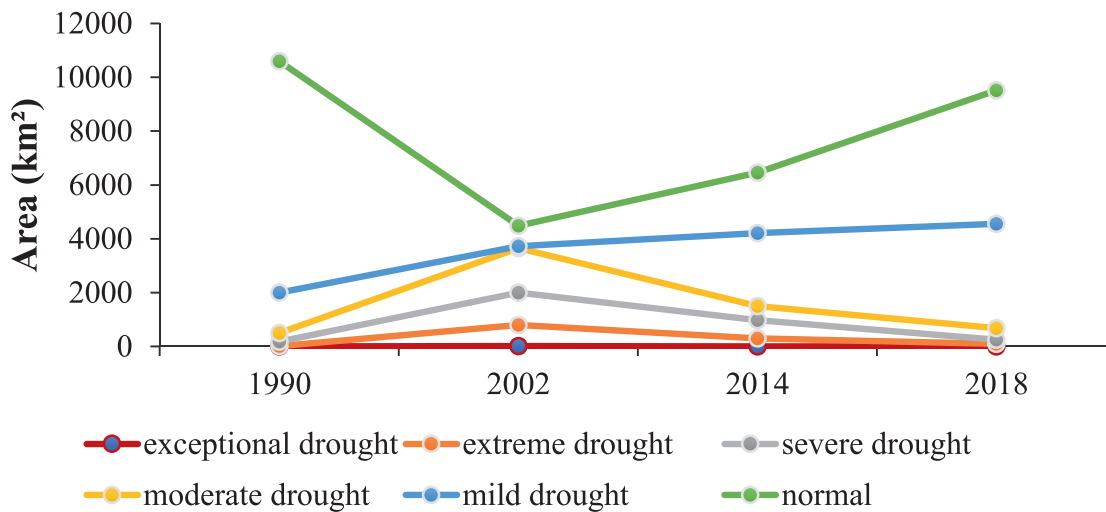


Fig. 12. Trends of drought pattern based on VSDI.

Table 8

Summary results of TVDI based drought in the years 1990, 2002, 2014, and 2018.

| Used Index | Drought Severity Class | 1990 Area (km ²) | Area (%) | 2002 Area (km ²) | Area (%) | 2014 Area (km ²) | Area (%) | 2018 Area (km ²) | Area (%) |
|------------|------------------------|------------------------------|----------|------------------------------|----------|------------------------------|----------|------------------------------|----------|
| TVDI | Very Wet | 16.48 | 0.10 | 0.21 | 0.00 | 44.28 | 0.27 | 80.61 | 0.50 |
| | Wet | 11355.55 | 70.34 | 1450.49 | 8.96 | 5470.5 | 33.80 | 9968.9 | 61.59 |
| | Normal | 4682.43 | 28.93 | 12140.6 | 75.01 | 9668.9 | 59.74 | 5340.59 | 33.00 |
| | Dry | 127.38 | 0.79 | 2516.17 | 15.55 | 979.35 | 6.05 | 782.89 | 4.84 |
| | Very Dry | 3.15 | 0.02 | 77.52 | 0.48 | 21.69 | 0.13 | 11.9 | 0.07 |

Table 9

Summary results of VSDI based drought in the years 1990, 2002, 2014, and 2018.

| Used Index | Drought Severity Class | 1990 Area (km ²) | Area (%) | 2002 Area (km ²) | Area (%) | 2014 Area (km ²) | Area (%) | 2018 Area (km ²) | Area (%) |
|------------|------------------------|------------------------------|----------|------------------------------|----------|------------------------------|----------|------------------------------|----------|
| VSDI | Exceptional | 1.94 | 0.01 | 19.54 | 0.12 | 3.24 | 0.02 | 2.38 | 0.01 |
| | Extreme | 50.32 | 0.31 | 900.34 | 5.56 | 505.49 | 3.12 | 100.23 | 0.62 |
| | Severe | 283.13 | 1.75 | 2400.7 | 14.83 | 1200.09 | 7.41 | 251.66 | 1.55 |
| | Moderate | 904.6 | 5.59 | 3954.6 | 24.43 | 1502.13 | 9.28 | 1547.99 | 9.56 |
| | Mild | 3000 | 18.54 | 3922.4 | 24.23 | 5409.1 | 33.42 | 4562.8 | 28.19 |
| | Normal | 11945 | 73.80 | 4987.41 | 30.82 | 7564.9 | 46.74 | 9719.93 | 60.06 |

the year 2002. No drought condition is maximum in the year of 1990 and minimum in 2014.

3.4. Temperature vegetation dryness index (TVDI)

Drought has been classified into five classes based on TVDI values such as very wet, wet, normal, dry, and very dry soil. Very few areas near the Tista River in Lalmonirhat indicate a very wet soil type which is 0.10% of the total study area in 1990 (Table 8). A large portion of all the districts especially Kurigram, Lalmonirhat, and Rangpur exhibits wet soil (70.34%) type. South-East corner of Gaibandha and Kurigram districts large area of Birampur Upazila, small portions of Thakurgaon, Panchagarh and Nilphamari districts experiences normal soil (28.93%) type. Sand bar of Brahmaputra and Dharla and Tista River express dry soil type (0.79%). Atrai and Karatoya River sand has very dry soil (0.02%) type this year. In 2002, South-West corner of Gaibandha, South-East corner and upper part of Dinajpur, scattered part of Thakurgaon, South-East corner of Panchagarh and Northern part of Lalmonirhat districts exposed dry soil (15.55%) type. Sand bar of Brahmaputra River expressed very dry soil (0.48%) type (Fig. 9).

In 2014, a small area near the Brahmaputra River of Kurigram districts represents a very wet soil (0.27%) type. A huge part of Kurigram,

Gaibandha, Rangpur, Thakurgaon, and Panchagarh districts and several parts of Nilphamari and Lalmonirhat districts characterize wet soil type (33.80%). The northern, central and southern part of the study area represents normal soil (59.74%) type. Sand Bar of Brahmaputra River in the Eastern part of the study area shows very dry soil (0.13%) type.

In 2018, very wet soil (0.50%) covers a minute area near Brahmaputra River in Kurigram district. Eastern districts (Kurigram, the lower part of Lalmonirhat, Gaibandha, Rangpur, and a large portion of Dinajpur) and several parts of Thakurgaon districts of the study area represents wet soil (61.59%) condition. A small portion in the upper part of Panchagarh, Western part of Thakurgaon, Eastern part of Dinajpur, and Western part of Rangpur characterize dry soil (4.84%). Dry sand of Tista (near the upper part of Lalmonirhat) and Brahmaputra (near the lower part of Gaibandha) rivers represents very dry soil (0.07%) type.

Very wet soil found a small percentage in each respective year. Wet soil type was maximum (70.34) in 1990 and a minimum (8.96%) in the year of 2002. It was average in the years 2014 and 2018. Results from the 2002 map indicate a maximum (75.01%) and 1990 indicates a minimum (28.93%) amount of normal soil type (Fig. 10). Among the years, dry soil type was highest (15.55%) in 2002 and lowest (0.79%) in the year 1990. All the year expresses a small amount of dry soil type.

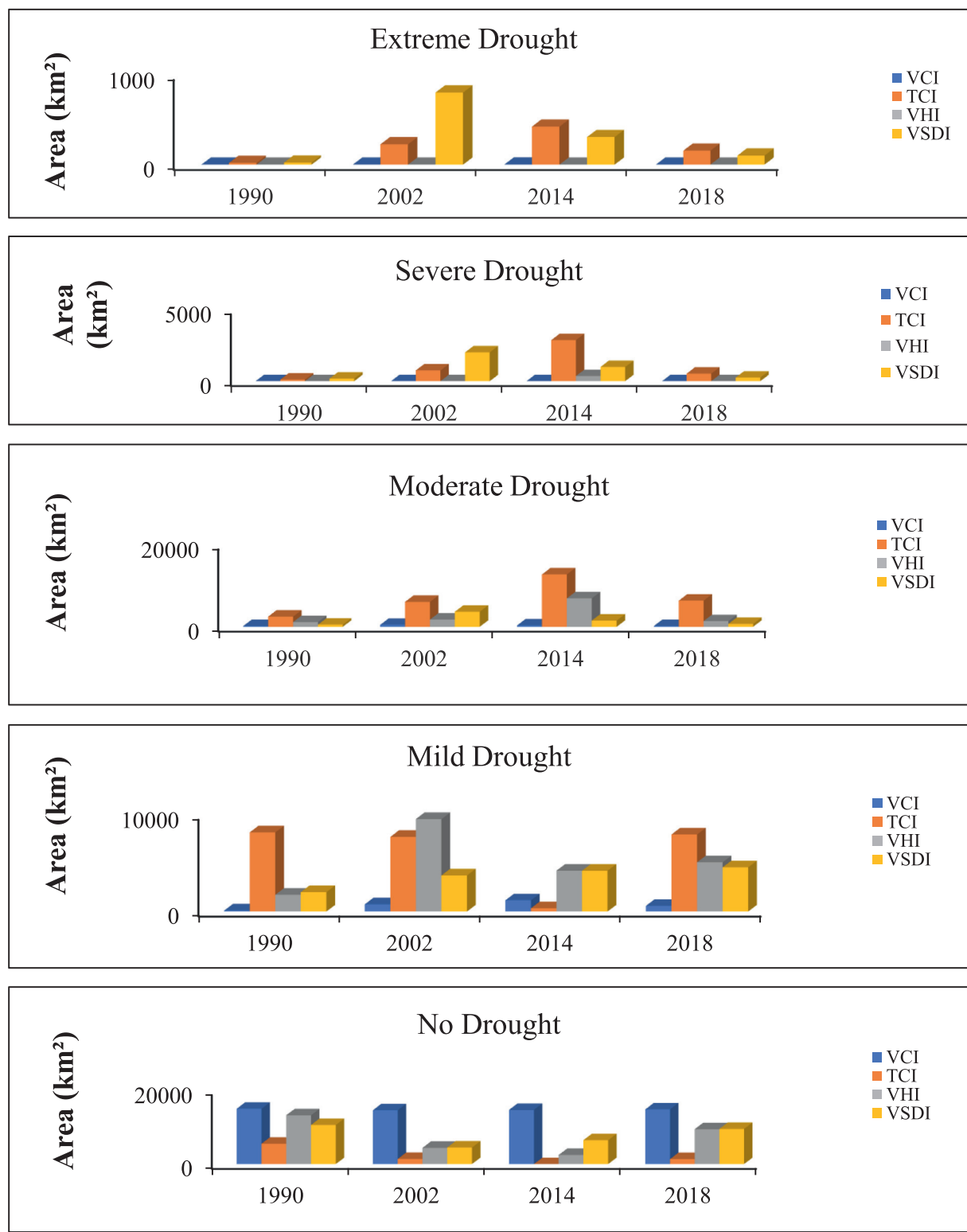


Fig. 13. Comparison among different drought indices (VCI, TCI, VHI, and VSDI).

3.5. Visible and shortwave infrared drought index (VSDI)

Drought has been classified into six classes based on VSDI values such as exceptional, extreme, severe, moderate, mild, and normal. The exceptional drought was almost absent (0.01%) in 1990. Extreme (0.31%) and severe drought (1.75%) class represent a small area which was

mainly the river (Kaatoya, Dharla, Atrai) sand bar. Dry sand of the Tista and Brahmaputra River indicates moderate drought (5.59%) condition (Table 9). The central districts (Dinajpur, Nilphamari, Rangpur) and upper part of Lalmonirhat district indicate mild drought (18.54%).

In 2002, exceptional drought represented very few areas which are only 0.12 % of the total study area. Dried river channeled (Tista,

GROUND SOIL MOISTURE POINTS OVER TVDI INDEX MAP (2018)

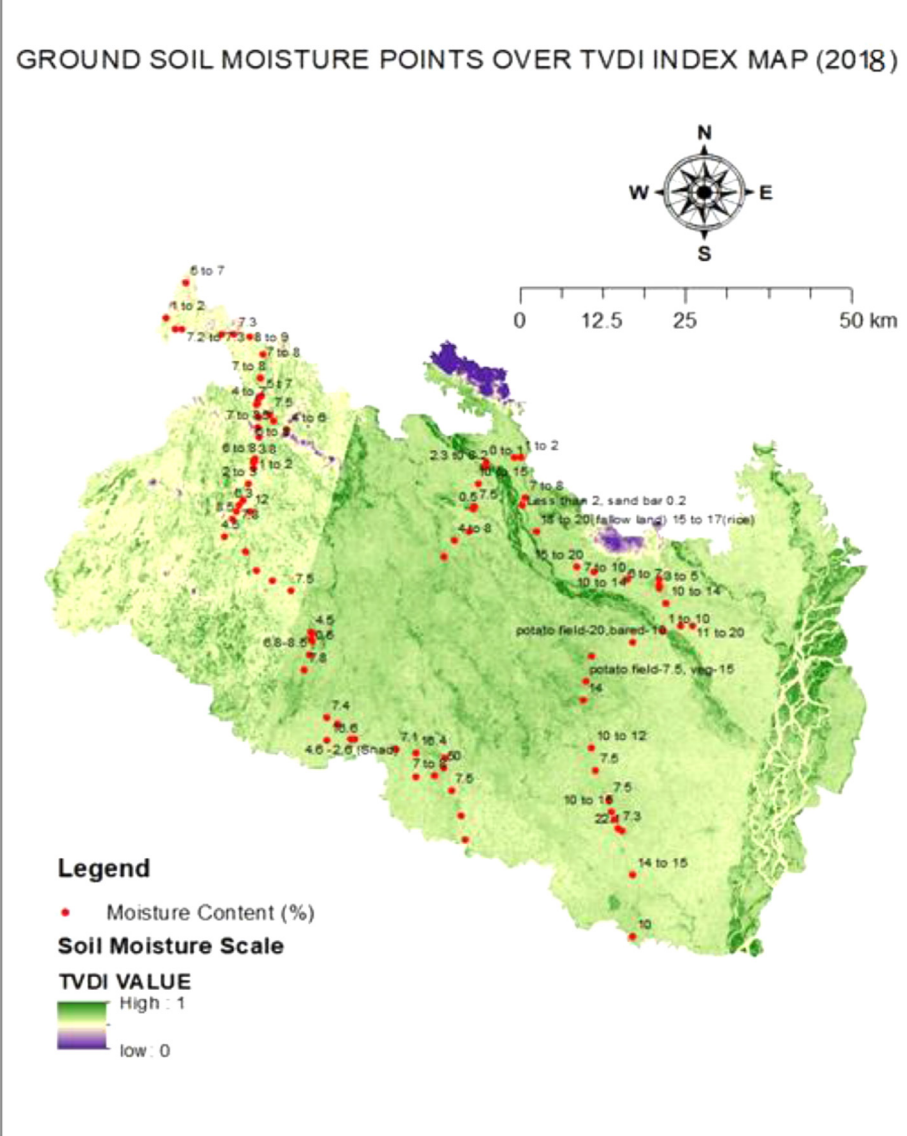


Fig. 14. Accuracy assessment using both the image-derived and ground collected soil moisture data.

Brahmaputra), some parts of Thakurgaon and Dinajpur districts expose to extreme drought (5.56%). Birampur Upazila and central part of Dinajpur district, most parts of Thakurgaon, Rangpur, and Nilphamari districts, few portions of Panchagarh and Lalmonirhat districts indicates severe drought (14.83%). A large portion of Nilphamari, Rangpur, Dinajpur, Thakurgaon, Panchagarh, and Lalmonirhat districts shows moderate drought (24.43%). Normal (30.82%) condition was found in the Eastern part of the study area. In 2014, exceptional drought was almost zero (0.02%). Sand bars of Brahmaputra and Tista River, several parts of Dinajpur Rangpur districts expose to extreme (3.12%) drought conditions (Fig. 11). The large area of Dinajpur and Rangpur and several areas of Thakurgaon districts subjects to severe (7.41%) drought. The southern and central part of Dinajpur, Eastern part of Panchagarh and Thakurgaon, Northern part of Lalmonirhat, and many parts of Nilphamari districts indicate moderate (9.28%) drought condition. In 2018, exceptional, extreme, and severe drought encompasses a small area which is only 0.01%, 0.62%, and 1.55% of the total study area respectively. Dried river channeled and few areas of northern Lalmonirhat represent severe drought. Several parts of Nilphamari, Dinajpur, Rangpur, and upper parts of Lalmonirhat districts indicate moderate (9.28%) drought conditions.

The year 2002 shows the highest amount of drought severity. Mild, moderate, severe and extreme condition is maximum and normal condition is minimum in 2002 (Fig. 12). The next drought-prone year is 2014 which indicates a higher amount of drought severity. The year 1990 represents the least drought-prone among all the years. This year, most of the area occupies normal conditions. Like 1990, much of the area in 2018 shows normal (60.06%) conditions.

3.6. Comparisons among the drought indices

In case of extreme drought, VCI indicates zero areas in all the years. TCI indicates a maximum area in 2014 (2.58%) and a minimum in 1990 (0.12%). VSDI prevails higher area in 2014 (5.45%) and a lower area in 1990 (0.17%). For severe drought, TCI specifies a maximum area in 2014 (17.49%) and minimum in 1990 (0.68%), VHI represents the higher area in 2014 (2.53%) and lower in rest of the year, VSDI indicates the highest area in 2002 (13.64%) and lowest in the year of 1990 (1.38%). Concerning moderate drought, VCI shows a maximum area in 2002 (2.90%) and a minimum area in 1990 (Fig. 13). TCI identifies a higher area in 2014 (77.84%) and a lower area in 1990 (15.13%). VHI shows the highest area in 2014 (49.53%) and the lowest area in 1990

Comparisiom between Moisture Content (Field Data Vs Image Derived)

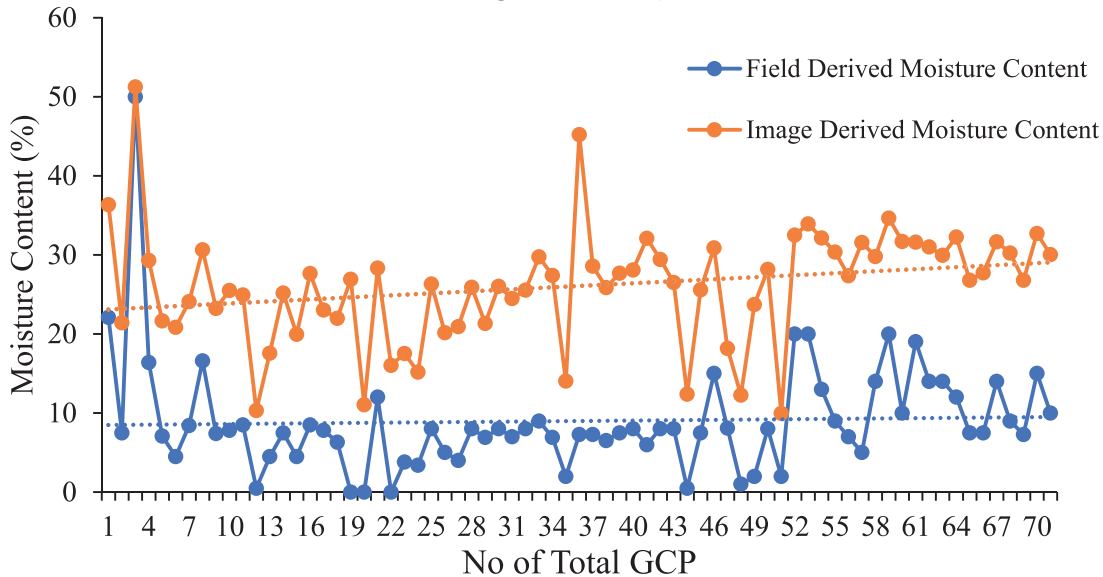


Fig. 15. Comparison between images derived and ground collected soil moisture data.

Relationship between TVDI and Relative Soil Moisture

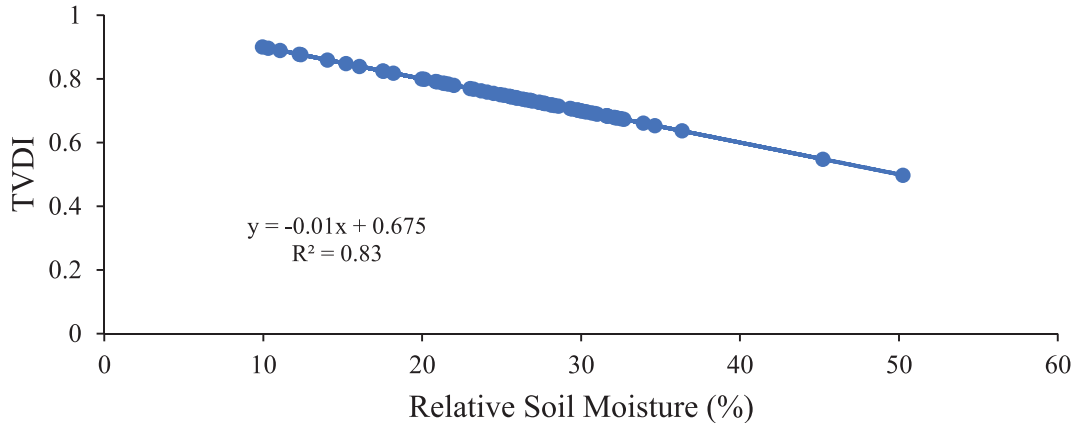


Fig. 16. Relationship between TVDI and Relative Soil Moisture.

(7.05%). VSDI represents the maximum area in 2002 (24.91%) and the minimum area in 1990 (3.76%).

In the case of mild drought, TCI holds the highest area in the year 1990 (50.18%) and the lowest area in 2014 (2.08%). VHI shows the maximum area in the year 2002 (60.87%) and the minimum area in 1990 (10.75%). VSDI represents the maximum area in 2014 (31.25%) and the minimum area in 1990 (15.04%). For no drought or normal condition, VCI indicates a higher amount of area in 1990 (98.24%) and lower in 2014 (90.90%) (Fig. 13). TCI shows a maximum area in 1990 (33.89%) and a minimum in 2014 (0.01%). VHI represents the highest area in 1990 (82.19%) and the tiniest area in 2014 (17.69%). VSDI occupies the largest area in 1990 (79.64%) and smallest area in 2002.

3.7. Accuracy assessment

To determine the precision of the soil moisture and LST from satellite images, an accuracy assessment has been performed (Fig. 14). The ground observation or ground truth data with the observed TVDI value from the analyzed satellite image has been taken as reference data. Field-

work has been done on the same date of image acquisition in the study area to verify image-derived soil moisture content. The study needed overall three Landsat scenes to cover the whole area and fieldwork has been conducted on the same scene acquisition date (11.11.2018, 11.11.2018, and 02.11.2018). The TVDI map of 2018 using Landsat data has been compared with these ground truth data and the accuracy assessment has been done. Both the field and image-derived data shows almost a similar trend (Fig. 15). TVDI and relative soil moisture show an inverse relationship (Fig. 16).

4. Discussion

The present study is the first attempt to use several drought indices for monitoring drought scenarios in northwestern Bangladesh. Many studies around the globe have used spatial analytical methods for drought monitoring (Zeng et al., 2019; Han et al., 2016; Hagenlocher et al., 2019; Wilhite et al., 2014). But the present study has a uniqueness as it has applied a combined approach of image and field-based observations of drought on a regional scale on a plainland

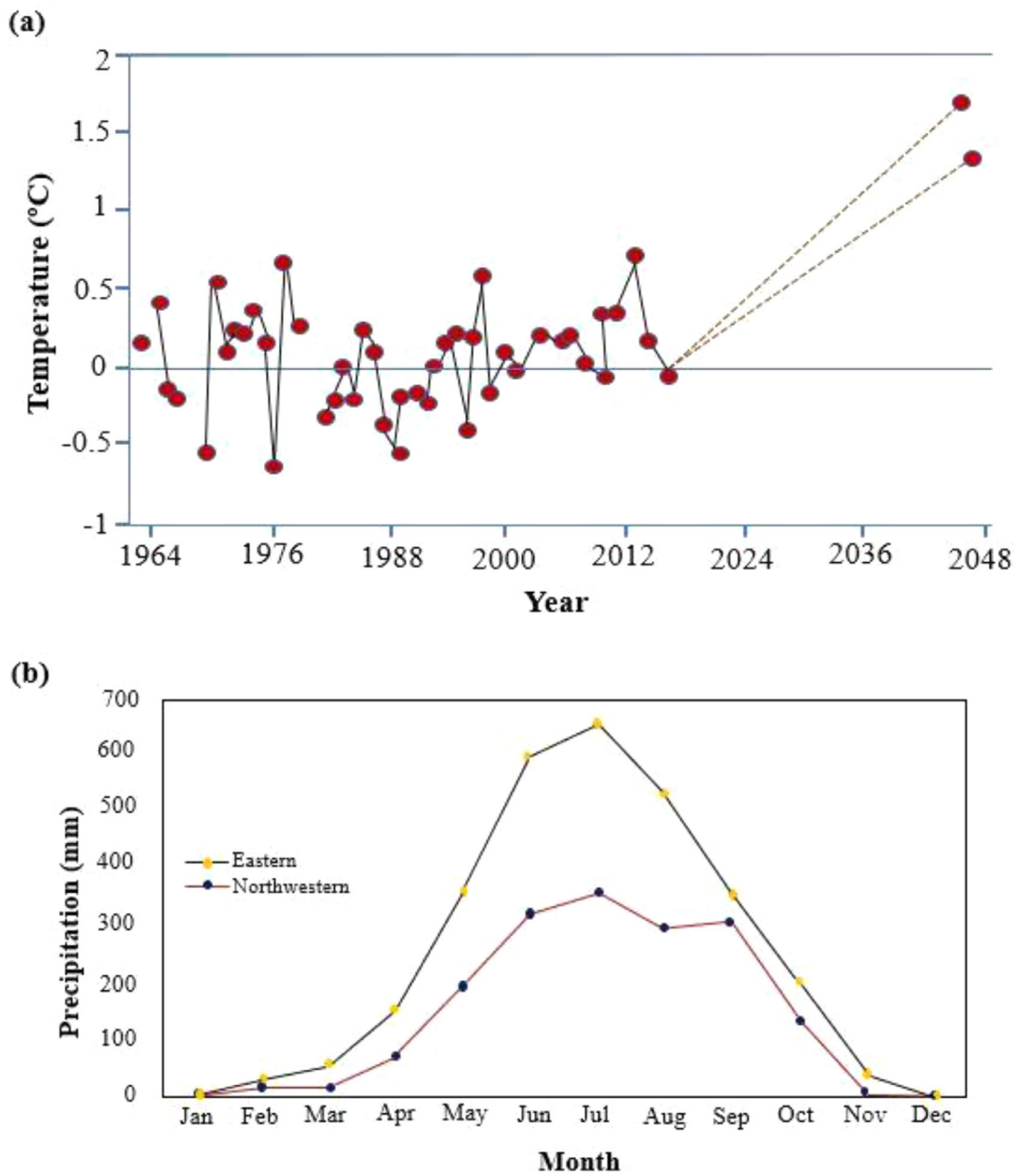


Fig. 17. (a) Variations of annual average maximum temperature from 1964 to 2018 and further projection up to 2048 in the northwestern part of Bangladesh; The two dashed lines portrays the lower and upper boundaries of the 2050 forecast, specify a probable temperature variation if global warming is continued. (b) Monthly distribution of precipitation from 1990 to 2018 in the eastern and northwestern part of Bangladesh. Data source: Bangladesh Metrological Department (BMD); Asian Disaster Preparedness Center (ADPC).

topography with sparse forest covers. Hence, this work will be a great contribution to the divisional and urban master plan for plummeting the ongoing crisis arising from droughts. Different drought indices measure drought using individual measuring parameters. Total area for different indices varied in different years due to the spatiotemporal change of these parameters (LST, ecological productivity, vegetation cover, vegetation health, soil moisture, urban growth) throughout the study time-frame. The VHI characterizes the health of the vegetation and combines VCI and TCI to detect vegetation conditions affected by drought (Kogan, 1997). TVDI is generally used to monitor drought levels based on LST and NDVI assuming land surface moisture (Han et al., 2010). From the comparisons among the indices and field validation, it is recommended that a combination of TVDI and VHI is the most suitable indices for this area on a regional scale. These two indices are very use-

ful to measure drought in a regional area similar to the present study area with huge vegetation cover including agricultural land and sparse urban structure.

The study is in agreement with some previous studies in the case of the identification of drought-prone areas (Shahid & Behrawan, 2008; Rahman & Latche, 2016). But the present study has a better reflection of drought occurrences due to the simultaneous consideration of soil moisture, LST, and LULC along with vegetation condition. Similar results also reported by another study conducted by Kamruzzaman et al. (2018) stated that in recent decades extreme drought prevalence increases in the northwestern part of Bangladesh compared to other regions. It is seeming that the study is based on the already established drought indices used by many researchers across the globe (Wu et al. 2020; Liu et al., 2016; Huang et al. 2015; Labedzki &

Bak, 2014), it is correspondingly crucial to consider the results impacted by the geographic variability like the study area.

Rai et al. (2017) accounted that nearly 60% land of Bangladesh is accessible for cultivation. However, a recent concern is that these cultivable lands are decreasing day by day throughout the country (Quasem 2011). In northwestern Bangladesh, this is due to the curse of severe drought conditions during the period of peak cultivation in this region. The drought pattern in this area has been induced huge changes in the land use land cover (LULC) as people are clearing the forest area for agricultural purposes, hence forest converting into agricultural land due to the increasing demand for meeting the production deficits. LST also playing a major role in the prevailing pattern of drought over the area (Akter et al., 2021). LST of the area is increasing due to the unplanned urbanization like in other parts of the country (Gazi et al. 2020; Tania et al. 2021) but the trend is alarming in this area. It was observed that river bar area identified as most drought-prone that is actually due to the drying out the existing river channels. River sand bar shows higher temperature and low moisture content because it reflects heat to the atmosphere from enriched sands deposited by the rivers (Kafy et al., 2020). The variability of annual rainfall and depletion of vegetation cover due to urbanization must be considered for planning sustainable farming in this area. The area has been experiencing the depletion of soil moisture and biomass reduction leading to the occurrence of drought resulting from both anthropogenic and climatic factors. The climatic aspects of Bangladesh changed throughout this century due to the raised levels of greenhouse gases. Drought-prone areas of Bangladesh are drier than 50 years ago and the current forecast proposes that the country will turn out to be hotter, and it will face recurrent droughts owing to these soared rainfall variations. The annual average rainfall in northwestern Bangladesh varying from the mean represents drought conditions (Fig. 17). From October to December, this area receives lower precipitation that affects the yields and critical reproductive stages of the Aman rice due to low soil moisture. Each year about 2.32 million ha Aman rice is harmed by the impacts of drought in the northwestern part of Bangladesh. This study has investigated the relationship between drought and field moisture content and land-use pattern. Based on the results of this study and the locations identified as drought-prone can be taken into account to future take steps to overcome the drought impacts by making a proper plan.

5. Conclusion

Based on drought indices, severe drought was found in the different parts of the study area. Due to this drought severity, most of the agricultural lands have been left uncultivated due to a lack of water or soil moisture. Regions with low to mild drought conditions need no additional drought reduction measures. However, for severe drought risk areas like northern Lalmonirhat, central Nilphamari, and Thakurgaon, the southern part of Dinajpur, and part of the Panchagarh districts, water shortage is a concerning issue for sustainable agricultural practices. Strengthening water resources infrastructure with available water supply during a dry spell is very crucial in these regions. In northwestern Bangladesh, protection of cultivated land, trans-basin water transfer strategies, and agricultural water-saving technology will assist to alleviate the impacts of drought severity. Besides, seasonal rainwater harvesting for agricultural use could bring progressive results in drought adaptation in this region. To implement sustainable drought policy, spatial impact, the geographical diversity of droughts, and influencing factors should be considered. The country meteorological department should extend the network weather stations in the identified drought risks regions to provide more localized seasonal forecasts to enhance decision-making. However, the results from the multiple drought indices can contribute to monitoring the onset of agricultural drought as an early warning system. Alteration of sowing and planting times, modification of agricultural practices, preservation agriculture, and zero tillage could effectively improve resilience toward the impacts of drought. Prospective researchers

will find information from the result of this study for solving local and regional drought problems.

Declaration of Competing Interest

We wish to confirm that there are no known conflicts of interest associated with this publication and there has been no significant financial support for this work that could have influenced its outcome.

Acknowledgments

We are profoundly grateful to the Ministry of Science and Technology, Bangladesh for funding this research. We must acknowledge Department of Geology, University of Dhaka for providing laboratory facilities to analyze with the licensed software.

References

- Abdrabbo, M.A., Farag, A., Abul-Soud, M., El-Mola, M.M., Moursy, F.S., Sadek, I.I., Hashem, F.A., Taqi, M.O., El-Desoky, W.M.S., Shawki, H.H., 2012. Utilization of satellite imagery for drought monitoring in Egypt. *World Rural Obs.* 4, 27–37.
- Adnan, S., 1993. Institutional Aspects of Flood Protection Programmes: November 1991–October 1992. Living without floods: lessons from the drought of 1992, p. 7.
- Akter, T., Gazi, M.Y., Mia, M., 2021. Assessment of land cover dynamics, land surface temperature, and heat island growth in Northwestern Bangladesh using Satellite Imagery. *Environ. Process.* 1–30.
- Almamalchy, Y.S., Al-Quraishi, A.M.F., Moradkhani, H., 2020. Agricultural drought monitoring over Iraq utilizing MODIS products. In: *Environmental Remote Sensing and GIS in Iraq*. Springer, Cham, pp. 253–278.
- Aswathi, P.V., Nikam, B.R., Chouksey, A., Aggarwal, S.P., 2018. Assessment and monitoring of agricultural droughts in Maharashtra using meteorological and remote sensing-based indices. *ISPRS Ann. Photogram.* *Remote Sens. Spatial Inf. Sci.* 5.
- Baniya, B., Tang, Q., Xu, X., Haile, G.G., Chhipi-Shrestha, G., 2019. Spatial and temporal variation of drought based on satellite derived vegetation condition index in Nepal from 1982–2015. *Sensors* 19, 430.
- BBS, 2011. Population and Housing Census, 2011. Bangladesh Bureau of Statistics (BBS). Ministry of Planning, Government of the People's Republic of Bangladesh, Dhaka.
- Caccamo, G., Chisholm, L.A., Bradstock, R.A., Puotinen, M.L., 2011. Assessing the sensitivity of MODIS to monitor drought in high biomass ecosystems. *Remote Sens. Environ.* 115, 2626–2639.
- Choi, M., Hur, Y., 2012. A microwave-optical/infrared disaggregation for improving spatial representation of soil moisture using AMSR-E and MODIS products. *Remote Sens. Environ.* 124, 259–269.
- Dai, M., Huang, S., Huang, Q., Leng, G., Guo, Y., Wang, L., Zheng, X., 2020. Assessing agricultural drought risk and its dynamic evolution characteristics. *Agric. Water Manag.* 231, 106003.
- Dhawale, R., Paul, S.K., 2018. A Comparative analysis of drought indices on vegetation through remote sensing for LATUR region of INDIA. *International Archives of the Photogrammetry, Remote Sens. Spatial Inf. Sci.*
- Dracup, J.A., Lee, K.S., Paulson Jr, E.G., 1980. On the definition of droughts. *Water Resour. Res.* 16 (2), 297–302.
- Gazi, M.Y., Rahman, M.Z., Uddin, M.M., Rahman, F.A., 2020. Spatio-temporal dynamic land cover changes and their impacts on the urban thermal environment in the Chittagong metropolitan area, Bangladesh. *GeoJournal.* 1–16. doi:10.1007/s10708-020-10178-4.
- Ghaleb, F., Mario, M., Sandra, A., 2015. Regional landsat-based drought monitoring from 1982 to 2014. *Climate* 3, 563–577.
- Hagenlocher, M., Meza, I., Anderson, C., Min, A., Renaud, F., Walz, Y., Siebert, S., Sebesvari, Z., 2019. Drought vulnerability and risk assessments: State of the art, persistent gaps, and research agenda. *Environ. Res.*
- Han, L., Zhang, Q., Ma, P., Jia, J., Wang, J., 2016. The spatial distribution characteristics of a comprehensive drought risk index in southwestern China and underlying causes. *Theor. Appl. Climatol.* 124, 517–528.
- Han, Y., Wang, Y., Zhao, Y., 2010. Estimating soil moisture conditions of the greater Changbai Mountains by land surface temperature and NDVI. *IEEE Trans. Geosci. Remote Sens.* 48, 2509–2515.
- Han, Z., Huang, Q., Huang, S., Leng, G., Bai, Q., Liang, H., Fang, W., 2021. Spatial-temporal dynamics of agricultural drought in the Loess Plateau under a changing environment: Characteristics and potential influencing factors. *Agric. Water Manag.* 244, 106540.
- Heim, R.R., 2002. A review of twentieth-century drought indices used in the united states. *Bull. Am. Meteorol. Soc.* 83, 1149–1165.
- Hossain, M., 1990. Natural calamities, instability in production and food policy in Bangladesh. *Bangladesh Develop. Stud.* 33–54.
- Huang, Y., Liu, X., Shen, Y., Liu, S., Sun, F., 2015. Advances in remote sensing derived agricultural drought monitoring indices and adaptability evaluation methods. *Trans. Chin. Soc. Agric. Eng.* 31, 186–195.
- Iglesias, A., Garrote, L., Cancelliere, A., Cubillo, F., Wilhite, A.D., 2009. Coping with drought risk in agriculture and water supply systems. In: *Drought Management and Policy Development in the Mediterranean*. Advances in Natural and Technological Hazards Research, p. 26.
- Islam, M.A., Miah, M.M., 1981. Bangladesh in maps. Univ. of Dacca 77 pp.

- Ji, L., Peters, A.J., 2003. Assessing vegetation response to drought in the northern Great Plains using vegetation and drought indices. *Remote Sens. Environ.* 87, 85–98.
- Kafy, A.A., Rahman, M.S., Hasan, M.M., Islam, M., 2020. Modelling future land use land cover changes and their impacts on land surface temperatures in Rajshahi. *Remote Sens. Appl. Soc. Environ.*
- Kamruzzaman, M., Kabir, M.E., Rahman, A.S., Jahan, C.S., Mazumder, Q.H., Rahman, M.S., 2018. Modeling of agricultural drought risk pattern using Markov chain and GIS in the western part of Bangladesh. *Environ. Develop. Sustain.* 20, 569–588.
- Kogan, F.N., 1997. Global drought watches from space. *Bull. Am. Meteorol. Soc.* 78, 621–636.
- Kogan, F.N., 2001. Operational space technology for global vegetation assessment. *Bull. Am. Meteorol. Soc.* 82, 1949–1964.
- Łabędzki, L., Bałk, B., 2014. Meteorological and agricultural drought indices used in drought monitoring in Poland: a review. *Meteorology Hydrology and Water Management. Res. Oper. Appl.* 2.
- Landsat 8 data user handbook, 2015. Department of the Interior U.S. Geological Survey, approved by K. Zanter, LSDS CCB Chair USGS, LSDS-1574 Version 1.0.
- Liu, X., Zhu, X., Pan, Y., Li, S., Liu, Y., Ma, Y., 2016. Agricultural drought monitoring: Progress, challenges, and prospects. *J. Geogr. Sci.* 26, 750–767.
- Liu, X., Zhu, X., Zhang, Q., Yang, T., Pan, Y., Sun, P., 2020. A remote sensing and artificial neural network-based integrated agricultural drought index: Index development and applications. *Catena* 186, 104394.
- Mahyou, H., Karrou, M., Mimouni, J., Mrabet, R., El Mourid, M., 2010. Drought risk assessment in pasture arid Morocco through remote sensing. *Afr. J. Environ. Sci. Technol.* 4, 845–852.
- Mishra, A.K., Singh, V.P., 2010. A review of drought concepts. *J. Hydrol.* 391, 202–216.
- Mladenova, I.E., Bolten, J.D., Crow, W., Sazib, N., Reynolds, C., 2020. Agricultural drought monitoring via the assimilation of SMAP soil moisture retrievals into a global soil water balance model. *Front. big Data* 3, 10.
- Mladenova, I.E., Jackson, T.J., Njoku, E., Bindlish, R., Chan, S., Cosh, M.H., Holmes, T.R.H., de Jeu, R.A.M., Jones, L., Kimball, J., 2014. Remote monitoring of soil moisture using passive microwave-based techniques—Theoretical basis and overview of selected algorithms for AMSR-E. *Remote Sens. Environ.* 144, 97–213.
- Murad, H., Islam, A.K.M.S., 2011. Drought assessment using remote sensing and GIS in north-west region of Bangladesh. In: Proceedings of the 3rd International Conference on Water & Flood Management, pp. 797–804.
- Neupane, M., Thakur, J.K., Gautam, A., Dhakal, A., Pahari, M., 2014. Arsenic aquifer sealing technology in wells: a sustainable mitigation option. *Water, Air, & Soil Pollution* 225, 2087.
- Padhee, S.K., Nikam, B.R., Dutta, S., Aggarwal, S.P., 2017. Using satellite-based soil moisture to detect and monitor spatiotemporal traces of agricultural drought over Bundelkhand region of India. *GIScience & Remote Sens.* 54, 144–166.
- Quasem, MA, 2011. Conversion of agricultural land to non-agricultural uses in Bangladesh: Extent and determinants. *Bangladesh Dev. Stud.* 34, 59–85.
- Rahman, M.R., Lateh, H., 2016. Meteorological drought in Bangladesh: assessing, analysing and hazard mapping using SPI, GIS and monthly rainfall data. *Environ. Earth Sci.* 75, 1–20.
- Rai, R., Zhang, Y., Paudel, B., Li, S., Khanal, N.R., 2017. A synthesis of studies on land use and land cover dynamics during 1930–2015 in Bangladesh. *Sustainability* 9, doi:10.3390/su9101866, 1866.
- Reiman, K.U., 1993. *Geology of Bangladesh. Tutte Druckerei Gmbh.*
- Rhee, J., Im, J., Carbone, G.J., 2010. Monitoring agricultural drought for arid and humid regions using multi-sensor remote sensing data. *Remote Sens. Environ.* 114, 2875–2887.
- Rojas, O., Vrieling, A., Rembold, F., 2011. Assessing drought probability for agricultural areas in Africa with coarse resolution remote sensing imagery. *Remote Sens. Environ.* 115, 343–352.
- Sandeep, P., Reddy, G.O., Jegankumar, R., Kumar, K.A., 2021. Monitoring of agricultural drought in semi-arid ecosystem of Peninsular India through indices derived from time-series CHIRPS and MODIS datasets. *Ecol. Indic.* 121, 107033.
- Sandholt, I., Rasmussen, K., Andersen, J., 2002. A simple interpretation of the surface temperature/vegetation index space for assessment of surface moisture status. *Remote Sens. Environ.* 79, 213–224.
- Seiler, R.A., Kogan, F., Wei, G., 2000. Monitoring weather impact and crop yield from NOAA AVHRR data in Argentina. *Adv. Space Res.* 26, 1177–1185.
- Shahid, S., Behrawan, H., 2008. Drought risk assessment in the western part of Bangladesh. *Nat. Hazards* 46, 391–413.
- Sholihah, R.I., Trisasantoko, B.H., Shiddiq, D., La Ode, S.I., Kusdaryanto, S., Panuju, D.R., 2016. Identification of agricultural drought extent based on vegetation health indices of landsat data: case of Subang and Karawang, Indonesia. *Procedia Environ. Sci.* 33, 14–20.
- Souza, A.G.S.S., Neto, A.R., de Souza, L.I., 2021. Soil Moisture-Based Index For Agricultural Drought Assessment: SMADI Application in Pernambuco State-Brazil, 252. *Remote Sensing of Environment*.
- , 2007. “Space Research and Remote Sensing Organization Bangladesh”. SPARRSO Newsletter, p. 20.
- Stathopoulou, M., Cartalis, C., 2007. Daytime urban heat islands from Landsat ETM+ and Corine land cover data: An application to major cities in Greece. *Solar Energy* 81, 358–368.
- Tania, A.H., Gazi, M.Y., Mia, M.B., 2021. Evaluation of water quantity-quality, floodplain landuse, and land surface temperature (LST) of Turag River in Bangladesh: an integrated approach of geospatial, field, and laboratory analyses. *SN Appl. Sci.* 3, 1–18.
- Tucker, C.J., Vanpraet, C., Boerwinkel, E., Gaston, E.A., 1983. Satellite remote sensing of total dry matter production in the Senegalese Sahel. *Remote Sens. Environ.* 13, 461–474.
- Vaani, N., Porchelvan, P., 2018. Monitoring of agricultural drought using fortnightly variation of vegetation condition index (VCI) for the State of Tamil Nadu, India. *International Archives of the Photogrammetry, Remote Sens. Spatial Inf. Sci.* 42, 4–9.
- Wilhite, D.A., 2005. *Drought and Water Crises: Science, Technology, And Management Issues*. Crc Press.
- Wilhite, D., Sivakumar, M., Pulwarty, R., 2014. Managing drought risk in a changing climate: The role of national drought policy. *Weather. Clim. Extrem.* 3, 4–13.
- World Bank, 2000. “Bangladesh Climate Change and Sustainable Development”, World Bank Report (No. 21104-BD).
- Wu, B., Ma, Z., Yan, N., 2020. Agricultural drought mitigating indices derived from the changes in drought characteristics. *Remote Sens. Environ.* 244, 111813.
- Yoon, D.H., Nam, W.H., Lee, H.J., Hong, E.M., Feng, S., Wardlow, B.D., Kim, D.E., 2020. Agricultural drought assessment in East Asia using satellite-based indices. *Remote Sensing* 12 (3), 444.
- Zeng, Z., Wu, W., Li, Z., Zhou, Y., Guo, Y., Huang, H., 2019. Agricultural drought risk assessment in Southwest China. *Water* 11, 1064.
- Zhang, A., Jia, G., 2013. Monitoring meteorological drought in semiarid regions using multi-sensor microwave remote sensing data. *Remote Sens. Environ.* 134, 12–23.
- Zhang, N., Hong, Y., Qin, Q., Liu, L., 2013. VSDI: a visible and shortwave infrared drought index for monitoring soil and vegetation moisture based on optical remote sensing. *Int. J. Remote Sens.* 34, 4585–4609.
- Zhang, Q., Xiao, M., Singh, V.P., Li, J., 2012. Regionalization and spatial changing properties of droughts across the Pearl River basin. *China. J. Hydrol.* 472, 355–366.
- Zhang, X., Susan Moran, M., Zhao, X., Liu, S., Zhou, T., Ponce-Campos, G.E., Liu, F., 2014. Impact of prolonged drought on rainfall use efficiency using MODIS data across China in the early 21st century. *Remote Sens. Environ.* 150, 188–197.
- Zhou, K., Li, J., Zhang, T., Kang, A., 2021. The use of combined soil moisture data to characterize agricultural drought conditions and the relationship among different drought types in China. *Agric. Water Manag.* 243, 106479.